



Published in final edited form as:

Annu Rev Biochem. 2019 June 20; 88: 163–190. doi:10.1146/annurev-biochem-013118-110644.

Redox Chemistry in the Genome: Emergence of the [4Fe4S] Cofactor in DNA Repair and Replication

Jacqueline K. Barton, Rebekah M. B. Silva, and Elizabeth O'Brien

Division of Chemistry and Chemical Engineering, California Institute of Technology, Pasadena CA 91125

Abstract

Many DNA-processing enzymes have been shown to contain a [4Fe4S] cluster, a common redox cofactor in biology. We find using DNA electrochemistry that binding of the DNA polyanion promotes a negative shift in [4Fe4S] cluster potential, which corresponds thermodynamically to ~500-fold increase in DNA binding affinity for the oxidized [4Fe4S]³⁺ cluster versus the reduced [4Fe4S]²⁺ cluster. This redox switch can be activated from a distance using DNA charge transport chemistry. DNA-processing proteins containing the [4Fe4S] cluster are enumerated with possible roles for the redox switch, highlighted. A model is described where repair proteins may signal one another using DNA-mediated charge transport as a first step in their search for lesions. The redox switch in eukaryotic DNA primases appears to regulate polymerase handoff, and in DNA polymerase δ , the redox switch provides a means to modulate replication in response to oxidative stress. Thus we describe redox signaling interactions of DNA-processing [4Fe4S] enzymes as well as the most interesting potential players to consider in delineating new DNA-mediated redox signaling networks.

Keywords

DNA charge transport; iron sulfur clusters; base excision repair; DNA primase; DNA polymerase; redox signaling; oxidative stress

I. Introduction

Iron sulfur clusters are modular, tunable metal cofactors found in all domains of life that serve as one-electron carriers operating over a wide range of physiological potentials, from approximately -500 mV vs. NHE to 300 mV vs. NHE (1–3). Cytosolic and membrane-bound proteins have been found to coordinate a cubane [4Fe4S] cluster at a range of redox potentials that vary depending on the local protein environment and solvent exposure (Figure 1) (4, 5). Found in the [4Fe4S]²⁺ resting state, high potential [4Fe4S] clusters, like those in high potential iron (HiPIP) proteins, can be oxidized to the [4Fe4S]³⁺ state and lower potential clusters, like those in ferredoxins, can be reduced to the [4Fe4S]⁺ state (6). These cofactors commonly mediate redox reactions in nitrogen fixation, photosynthesis, and respiration (7–9), often acting in a chain of metal cofactors within an otherwise insulating protein matrix (10, 11).

Thirty years ago, these [4Fe4S] clusters were found also to be associated with a protein involved in DNA repair (12), and over time, more and more proteins involved in DNA processing were found to contain [4Fe4S] clusters. What were their roles? Were they structural factors or perhaps ancestral relics? As described here, we are finding that these [4Fe4S] clusters carry out redox reactions in DNA-processing proteins, serving as redox switches to regulate binding to the DNA polyanion.

[4Fe4S] Cluster Biogenesis and Loading to Target Proteins

After decades of progress, it is now understood that the incorporation of [4Fe4S] cofactors occurs through a highly regulated and coordinated series of metabolically expensive steps by a network of iron sulfur cluster biogenesis proteins (13–19). General biogenesis is carried out by the ISC pathway (Figure 2), where free iron and reduced sulfide (S^{2-} , derived from free cysteine) are scaffolded onto components of biogenesis machinery, delivered, and loaded to apo-protein targets in a process facilitated by chaperone proteins and driven by ATP hydrolysis. In prokaryotes, this entire process occurs within the cytosol. In eukaryotes, biogenesis begins in the mitochondria, and for cytoplasmic and nuclear-bound cluster proteins (which include repair and replication enzymes), is completed in the cytoplasm by the cytosolic iron sulfur assembly (CIA) machinery (16). At present, specialized biogenesis components have not been identified for [4Fe4S] repair proteins in prokaryotes. However, prokaryotic biogenesis has been linked to pathogenesis and antibiotic resistance (20). Future studies will likely be quite informative for uncovering new regulatory roles for FeS biogenesis in all domains of life.

Mechanisms of protein target recognition by biogenesis machinery have been brought to the forefront recently. Bioinformatic signatures of the coordinating cysteines in repair and replication proteins are surprisingly weak (21); however, newly discovered target sequences recognized by biogenesis machinery, which include an LYR motif and a KKK_{6–10}KK sequence, have been found to be essential for association with an ISC co-chaperone in yeast (13). Continued investigation of recognition motifs will be important for understanding cluster biogenesis, unraveling new facets in iron metabolism, and identifying new cluster proteins, such as those involved in DNA processes.

DNA-Processing [4Fe4S] Enzymes

The surprising discovery of a [4Fe4S] cluster in the base excision repair (BER) glycosylase Endonuclease III (EndoIII) from *Escherichia coli* (*E. coli*) in 1989 (12) soon led to the discovery of [4Fe4S] clusters in MutY (an EndoIII paralog) and Uracil DNA Glycosylase in *Archaeoglobus fulgidus* (AfUDG) (22, 23). Over the following decades, nucleic acid processing enzymes across several pathways were shown to contain [4Fe4S] cofactors (Table 1) (24–30). In most cases, discovery of the [4Fe4S] cluster occurred years after the first isolation of the gene products (27). As predictive tools and protein isolation methods become more and more sophisticated, we and others expect that even more [4Fe4S] clusters will be observed in essential DNA processing enzymes (27, 31).

The question of what role the [4Fe4S] clusters played, however, was less straightforward to answer, as early studies demonstrated that the clusters were isolated in the electron

paramagnetic resonance (EPR) silent $[4\text{Fe}4\text{S}]^{2+}$ state and resistant to powerful chemical oxidants and reductants (12, 23, 32). Moreover, the spectroscopic signature of coordinating cysteines was unchanged upon binding a damaged substrate, leading to the initial conclusion that the cluster had a structural role (12, 33, 34). MutY, however, could be denatured and refolded in the apo form, challenging this early conclusion (35). A substrate-sensing role was proposed for the cluster in light of this result, but a general, chemical function for the cofactor eluded observation.

II. Characterizing the Fundamental Properties of DNA-Mediated Charge Transport

In addition to the metabolic expense undertaken by cells to load a cluster into a target protein, placing an iron-containing cofactor in a DNA-binding enzyme can put the bound nucleic acid at risk of damage. A labile ferrous iron from the cofactor can undergo Fenton chemistry, creating reactive oxygen species and damaging nearby DNA bases (Figure 1) (36). Why then does Nature spend the requisite energy incorporating a redox-active inorganic cofactor into a DNA-processing enzyme?

At the same time that these proteins involved in DNA processing were being found to contain $[4\text{Fe}4\text{S}]$ clusters, experiments were being conducted to characterize DNA charge transport chemistry (DNA CT), where electrons rapidly migrate through well stacked duplex DNA (37). The native substrate of these $[4\text{Fe}4\text{S}]$ enzymes, double stranded DNA (dsDNA), was initially predicted to conduct charge in the dry, solid state (38), as the π -stacked DNA bases resemble the structure of graphite, a conductive material (Figure 3). To assess whether DNA conducted charge in biologically relevant aqueous conditions, new platforms were developed to examine this chemistry. Two important characteristics of this chemistry emerged: (i) DNA CT can occur over long molecular distances with shallow distance dependence, and (ii) DNA CT is exquisitely sensitive to perturbations in π -stacking of the bases.

A range of studies using DNA-bound electron donors and acceptors were used to characterize DNA CT chemistry. In an early photophysical study, a DNA oligomer was prepared containing a tethered luminescent ruthenium intercalator at one end and an intercalating rhodium oxidant at the other. While the tethered, DNA-bound ruthenium complex luminesced in the absence of the rhodium complex, in its presence, the luminescence of the ruthenium complex was quenched by electron transfer, remarkably over a distance $> 40 \text{ \AA}$ (39). In a subsequent experiment using ethidium as the luminescent donor, electron transfer quenching was also evident but was attenuated in the presence of a single base mismatch intervening between the bound ethidium and rhodium (40). Long-range CT through a 63 bp duplex DNA substrate has been observed with DNA-intercalating photooxidants, where the DNA-bound photooxidant can promote oxidative damage at guanine residues from a distance. A covalent rhodium photooxidant at one end of a DNA duplex, for example, oxidizes guanine bases at the 5'-guanine of a guanine doublet, the site of low oxidation potential, through DNA CT, generating 7,8-dihydro-8-oxo-2'-deoxyguanosine lesions 200 \AA from the site of intercalation (41). Experiments monitoring

base-base CT utilizing 2-aminopurine furthermore showed that these DNA CT reactions can occur on the picosecond timescale, gated by the motions of the bases (42), and moving 10 times the single-step tunneling distance through protein in a miniscule fraction of the time (10, 11, 37, 43, 44)!

Again, however, perturbations in base stacking, as occur with base mismatches or kinks in the DNA, turn off this long range CT chemistry. In fact, proteins that bind and kink the DNA, such as TATA-binding protein, can be used to turn off DNA CT. In contrast, proteins that bind DNA without affecting DNA base stacking, as with histones, do not alter DNA CT (45–47).

We also explored DNA CT in the ground state using DNA electrochemistry. Here, as with the photophysical studies, we observe long range CT as long as the DNA is well stacked. Indeed, ground state CT through DNA was observed over 100 base pairs to a tethered, intercalating redox probe, methylene blue, using DNA-modified gold electrodes, but a single base mismatch in the 100-mer was sufficient to attenuate the redox signal severely (48).

III. Measuring Redox Potentials of [4Fe4S] Enzymes Bound to DNA

For our early electrochemistry studies, we had used proteins to modulate DNA CT to a small DNA-bound redox probe (46), but we considered that DNA electrochemistry could be used also to examine DNA CT to a redox cofactor *within* a DNA-bound protein. Could a DNA-binding protein containing a redox cofactor carry out DNA CT chemistry? If so, DNA CT experiments could be used to characterize the redox centers of DNA-binding proteins and to determine their DNA-bound potentials.

DNA-Mediated Electrochemistry

DNA-modified Au electrodes have become a useful platform for assessing whether a DNA-processing, [4Fe4S] enzyme is redox-active in solution under physiologically relevant conditions (Figure 4). Gold surfaces are functionalized with alkanethiol-modified DNA duplexes through formation of a thiol-gold bond. The Au can be used as the working electrode in a three-electrode cell after surface washing and passivation (48–50). DNA-bound redox potentials of [4Fe4S] proteins can be measured with this method, where charge flows from the electrode through the DNA to the cluster. In this platform, the DNA, functionalized onto an electrode surface, is biologically accessible; restriction enzymes, for example, can cut the DNA on the electrode with sequence specificity, as in solution. Electrochemical studies on these platforms have been central to the prediction and discovery of redox signaling between DNA-bound [4Fe4S] enzymes across different repair pathways (51–53).

We first examined MutY, EndoIII, and AfUDG, the three base excision repair proteins found to contain [4Fe4S] clusters (32). Earlier studies using strong chemical oxidants and reductants had suggested that the clusters were redox-inactive at physiological potentials, but these studies had been conducted in the *absence* of DNA. It was reasonable to consider that binding the DNA polyanion might change the potential of the cluster within the protein. Our studies showed first that a reversible signal was detectable at ~80 mV versus NHE,

within the physiological window, for each of these proteins bound to the DNA-modified electrode. The potentials were consistent with those found for the clusters in HiPIP proteins and were at equal potentials for all of the repair proteins examined. Moreover, the presence of an abasic site on the DNA intervening between the bound protein and the electrode surface served to attenuate the signal from the cluster. This result established two important points: (i) we were measuring the *DNA-bound* potential of the protein and (ii) we were observing DNA-mediated CT between the electrode and the cluster within the protein. Many repair and replication proteins have now been studied using this DNA electrochemistry platform, and in each case we have observed reversible, redox signals in the physiological potential range, near ~ 80 mV vs. NHE, corresponding to cycling between the $[4\text{Fe}4\text{S}]^{2+}$ and $[4\text{Fe}4\text{S}]^{3+}$ oxidation states (28, 32, 51, 52, 54–57).

It is noteworthy that the most recent generation of DNA-modified electrodes utilizes a multiplexed chip so multiple experimental conditions can be examined in parallel (Figure 4) (48–50). Patterned, silicon chips with sixteen independently addressable Au electrodes uniform in area can be physically divided into four quadrants and used to monitor the redox activity of a single protein on as many as four different DNA substrates on the same surface. The platform can also be used to compare CT efficiency of WT and mutant protein on the same chip. All of the experiments described can moreover be carried out under strictly anaerobic conditions.

Graphite Electrochemistry to Compare DNA-bound and DNA-free $[4\text{Fe}4\text{S}]$ Cluster Potentials

We became interested in monitoring directly the shift in potential for $[4\text{Fe}4\text{S}]$ repair proteins associated with binding DNA, and that required measuring the protein potential both in the absence and presence of DNA. DNA electrochemistry on Au electrode surfaces is amenable to measuring physiological potentials ranging from -200 mV to $+500$ mV vs. NHE (28, 50–59). However, scanning beyond this range is necessary to observe a redox signal from a protein in the absence of DNA, which has a higher (more reductive) midpoint potential due to the absence of the DNA polyanion (51, 53, 56, 60, 61). In order to measure the DNA-free and DNA-bound redox potentials of EndoIII, highly oriented pyrolytic graphite (HOPG) electrodes were used (60). Bare surfaces or surfaces modified with pyrene-functionalized duplex DNA (which creates a DNA monolayer through π stacking between pyrene and graphite) facilitated direct comparison of DNA-free and DNA-bound EndoIII $[4\text{Fe}4\text{S}]$ cluster redox potentials. A negative shift of approximately 200 mV was observed for the DNA-bound EndoIII relative to DNA-free EndoIII. Given that protein binding importantly does not lead to a large conformational change in the protein or DNA, this shift in redox potential for the $[4\text{Fe}4\text{S}]$ cluster thermodynamically reflects a roughly 500-fold tighter DNA binding affinity for the oxidized $[4\text{Fe}4\text{S}]^{3+}$ state, relative to the reduced $[4\text{Fe}4\text{S}]^{2+}$ state, based on the Nernst equation (Figure 5). Oxidation of the $[4\text{Fe}4\text{S}]^{2+}$ cluster to the $[4\text{Fe}4\text{S}]^{3+}$ state thus should serve as a redox switch for DNA binding.

Spectroscopic Observation of $[4\text{Fe}4\text{S}]$ Cluster Redox Activity in DNA-Processing Proteins

Electrochemical observations of the $[4\text{Fe}4\text{S}]$ clusters in DNA-processing enzymes was also complemented by spectroscopic analysis. EPR spectroscopy requires chemical or

electrochemical conversion of the resting, diamagnetic $[4\text{Fe}4\text{S}]^{2+}$ enzymes to the paramagnetic oxidized $[4\text{Fe}4\text{S}]^{3+}$ or reduced $[4\text{Fe}4\text{S}]^+$ redox states, and thus was used to establish the resting state for the DNA-bound repair protein as $[4\text{Fe}4\text{S}]^{2+}$ (28, 62–65). We also demonstrated that the DNA-bound protein can be oxidized photochemically, from a distance, using DNA CT from a distantly tethered intercalating photooxidant (32, 51). Importantly, we were also able to demonstrate spectroscopically that the cluster could be oxidized by guanine radicals, generated using flash-quench experiments monitored by transient absorption spectroscopy (66). Indeed, these studies highlight how the oxidized $[4\text{Fe}4\text{S}]^{3+}$ cluster could be generated within the cell, *from a distance* using DNA CT from guanine radicals under conditions of oxidative stress, and in so doing, activating the DNA repair machinery.

IV. A Shift in Cluster Potential Reflects a Redox Switch in DNA Binding

While we had seen several examples of DNA binding yielding a shift in redox potential for the clusters within the repair proteins, from which one can infer a difference in DNA binding affinity for the protein with a $[4\text{Fe}4\text{S}]^{3+}$ cluster versus a $[4\text{Fe}4\text{S}]^{2+}$ cluster, we were not at first able to measure this difference directly. In the absence of DNA, the $[4\text{Fe}4\text{S}]^{3+}$ cluster degrades further to a $[3\text{Fe}4\text{S}]^+$ cluster, which affects protein binding. As a result, binding affinities for the $[4\text{Fe}4\text{S}]^{3+/2+}$ clusters needed to be determined anaerobically.

Recently we found that microscale thermophoresis could be used under anaerobic conditions to carry out DNA binding experiments for the $[4\text{Fe}4\text{S}]$ proteins in the two oxidation states. EndoIII containing the $[4\text{Fe}4\text{S}]^{3+}$ cluster was first generated on DNA-modified electrodes and then, under strictly anaerobic conditions, the thermophoresis experiments were conducted (53). Consistent with the shift in potential associated with DNA binding, oxidized EndoIII with the $[4\text{Fe}4\text{S}]^{3+}$ cluster was indeed found to bind >500 times more tightly to dsDNA than the reduced EndoIII with the $[4\text{Fe}4\text{S}]^{2+}$ cluster (Figure 5). This difference in binding affinity is understandable based simply on electrostatic considerations. In fact, calculations based upon the distance of the cluster to the DNA polyanion and the intervening protein dielectric well reflect the change in binding affinity that we see. It is interesting in that context that we find similar shifts in potential for all of the DNA repair proteins examined, and the clusters generally appear to be ~ 20 Å from the polyanionic DNA backbone. Based upon these results, then, we can consider that binding of these repair proteins to the DNA polyanion serves to tune the potential of the cluster by altering the electrostatic environment, activating the cluster toward oxidation and lowering the $[4\text{Fe}4\text{S}]^{3+/2+}$ couple into a physiologically accessible potential range.

V. $[4\text{Fe}4\text{S}]$ Proteins in Nucleic Acid Processing and Repair

Thousands of DNA damage sites are generated by endogenous and exogenous agents in each cell daily (67, 68). An arsenal of DNA repair pathways have evolved to address the structurally and chemically diverse lesions, though a comprehensive understanding of how repair pathways efficiently identify and remove damaged bases has remained elusive (69, 70). In the case of the repair proteins that contain $[4\text{Fe}4\text{S}]$ clusters, what they share is a low copy number within the cell and a moderate specificity in binding their target lesion versus

unmodified DNA. But with few players and not a high specificity in targeting, how do they effectively find all the lesions within the cell on a timescale appropriate to the organism?

We have considered that DNA charge transport chemistry might provide a first step in localizing repair proteins that contain these clusters in the vicinity of lesions, essentially redistributing the proteins to regions of damage, irrespective of the actual lesion characteristics as long as the damage interferes with DNA CT. We had actually found earlier that many common base lesions interfere with DNA CT (71). Moreover, the fact that these proteins share a similar redox potential means that essentially they can work together, transferring electrons from one to another to carry out a first scan of the genome.

A Model for Scanning the Genome Utilizing DNA CT Chemistry

To describe how DNA-mediated CT chemistry could be utilized for more efficient lesion detection, we developed a model for redox signaling among a network of [4Fe4S] repair proteins (Figure 6) (32). Upon association of freely-diffusing protein in the [4Fe4S]²⁺ state onto duplex DNA, the protein is activated toward oxidation and can reduce a distally bound protein from the [4Fe4S]³⁺ state to the more weakly binding [4Fe4S]²⁺ state (Figure 5, top). Alternatively, guanine radicals (G^{•+}), a product of oxidative stress, can generate the [4Fe4S]³⁺ species by DNA CT over long molecular distances (41, 66, 72). Iterations of this scanning can occur throughout the cell. However, if there is an intervening region of dsDNA containing a lesion that attenuates CT, redox signaling between the cluster proteins is interrupted. Both proteins in the tightly-binding [4Fe4S]³⁺ state persist on the DNA and can then localize to the precise site of damage (Figure 5, bottom).

We have, by now, found many types of DNA repair proteins containing [4Fe4S] clusters that are involved in redox signaling on DNA, and we have probed how these redox signaling networks work cooperatively utilizing DNA CT through their [4Fe4S] clusters. We have also found CT deficiencies in mutated proteins strongly linked to disease. In the context of redox signaling, included below is an overview of the major repair protein families that coordinate a [4Fe4S] cluster, and illustrations of how they may utilize redox signaling.

Glycosylases

Glycosylases are key players in BER, a highly conserved pathway responsible for recognizing and removing single-base lesions generated by spontaneous deamination, alkylating agents, and oxidative stress, among other sources of damage (Figure 7) (73, 74). For EndoIII, MutY, and AfUDG, biochemical studies have very elegantly demonstrated that mutations at coordinating cysteines or in the cluster binding domain can affect protein expression, enzymatic function, and DNA binding, even though the cluster is located remotely from the glycosylase active site and there is not a large conformational change associated with the binding to DNA (34, 75–77). Specific to mammalian BER, a connection has been established between the glycosylases, NTHL1 and MUTYH, and multiple cancers, most notably MUTYH-associated polyposis (MAP). These syndromes are characterized by increased risk of aggressive, early-onset colorectal cancer (68, 74, 78).

As described above, several BER glycosylases were demonstrated to participate in DNA-mediated CT chemistry (32). Further examination of the available structures of EndoIII in

the free and DNA-bound forms revealed a pathway of aromatic residues between the cluster and the DNA, separated by 15-20 Å, and predicted to provide a CT pathway (10, 11, 79, 80). Informed by these crystal structures, several key mutants of EndoIII have been generated and characterized, including a CT deficient/enzymatically proficient mutant Y82A, a complementary CT proficient but enzymatically deficient mutant D138A, and charge-flipped mutants to explore the electrostatics near the cluster (61, 79, 80). Unique to the HiPIP-like [4Fe4S] repair proteins, the DNA polyanion is the governing factor that shifts the potential and stabilizes the cluster in the [4Fe4S]³⁺ state (5, 61). Furthermore, redox sensing of base stacking perturbations on DNA-modified gold electrodes containing a lesion has been observed, even when that lesion is not a substrate for the glycosylase (32, 80).

Superfamily 2 (SF2) 5' → 3' Helicases

SF2 helicases were the second family of enzymes discovered to coordinate a [4Fe4S] cluster (65). SF2 helicases are NTP-dependent proteins that directionally translocate and unwind duplexes (81). Distinct from the glycosylase family, the FeS helicases are involved in several repair pathways (Figure 7). These pathways respond to stress from multiple sources, and there are many examples of extensive crosstalk and cooperativity among a complex network of repair pathways that include SF2 helicases with [4Fe4S] clusters (27). As might be expected, mutations in SF2 helicases containing [4Fe4S] clusters are associated with a host of genetic disorders and cancers and are being targeted for cancer therapies (82, 83).

A common theme with SF2 helicases is the multifunctional nature of their activities within the cell (Figure 7). In bacteria, DinG resolves R-loops, RNA:DNA hybrids formed at collisions between replication and transcription machinery; DinG has also been shown to be active on D-loops (displacement loops, triple stranded DNA) (64, 84). Notably, cysteine mutants of DinG are more susceptible to proteolytic degradation *in vitro* (64). A new, well-conserved bacterial protein YoaA, was identified in a genetics screen to be involved in coordinating repair and replication machinery at blocked replication forks. Based on sequence similarity to DinG, YoaA was predicted to be a [4Fe4S] protein (85).

The first archaeal/eukaryotic [4Fe4S] SF2 helicase discovered, XPD, is part of the transcription factor II H (TFIIH) complex and is involved in both nucleotide excision repair (NER) and transcription initiation (65). In NER, helicase activity is critical for removing damaged oligomers, which can be disrupted by mutating coordinating cysteines. In contrast, only the association of XPD with TFIIH is needed to initiate transcription, which is thought to aid assembly of other proteins with TFIIH. Many other facets of the XPD have also been studied, including regulation of XPD by other proteins, the timing of cluster insertion relative to XPD incorporation with TFIIH, how XPD is involved in cell cycle control, and a role for XPD in preventing oxidative damage in the mitochondria (86).

Both XPD and DinG can participate in DNA CT chemistry with a shared DNA-bound redox potential of approximately 80 mV vs. NHE and sense signal attenuating lesions (54, 59). Further probing of the CT activity found that upon addition of ATP, the signal for XPD and DinG quite stunningly increases in a concentration-dependent manner without any shift in the midpoint potential. Helicase activity thus increases the electrochemical signal through better coupling of the cluster to the π -stacked DNA bases, essentially signaling the helicase

activity through DNA CT. The increased coupling upon cofactor binding appears to be an important feature of the SF2 helicase family that helps coordinate repair and replication, and signaling from a distance that the helicase is active.

Another eukaryotic SF2 helicase, FANCI has a role in several pathways; compromised FANCI function, which can result from mutations in the cluster binding domain, has been linked to several cancers, and FANCI upregulation has been found in many tumor types (87). FANCI is known to act on many substrates, including duplex substrates, D-loops and G4 quadruplexes (87). FANCI association with numerous other proteins, including BRCA1, can depend on the timing of the damage response and the type of lesions generated. Furthermore, FANCI activity has been observed to alleviate replication stress through resolution of stalled replication forks, and particularly at telomeres rich in G4 quadruplexes. Two other SF2 helicases that coordinate a [4Fe4S] cluster, RTEL1 and Chl1, resolve several different types of structures in the process of facilitating replication (83, 88). Both RTEL1 and Chl1 have been also found to associate with various replication proteins. Mutations in these enzymes are similarly associated with an array of diseases (88, 89). Electrochemical studies of these proteins have not yet been conducted, but studying these proteins in the context of redox signaling will likely illuminate how these multifunctional enzymes may coordinate their activities.

Helicase-Nucleases

In 2009, the first helicase-nuclease containing a [4Fe4S] cluster identified was AddB, part of the AddAB heterodimer found in gram positive bacteria and some proteobacteria (90, 91). Helicase-nuclease activity is involved in double strand break (DSB) repair, which can be caused by several factors, including collapsed replication forks. Located in the C-terminal nuclease domain of AddB, the cluster was found to be essential for binding of DNA substrates, but not essential for complexation with AddA or for maintaining structure, though a stabilizing role of the cluster was suggested. The crystal structure of the AddAB in complex with a DNA substrate revealed a DNA binding loop supported by the cluster domain, providing explanation of why mutating coordinating cysteines abolished substrate binding (92). A homologous [4Fe4S] helicase-nuclease, Dna2, was later found in eukaryotes (*vide infra*).

Excision Nucleases

UvrC, an excision nuclease from *E. coli*, was reported in 2018 to be a [4Fe4S] protein (28). Only found in bacterial and some archaeal NER pathways, UvrC (in complex with another NER protein, UvrB) uniquely catalyzes incisions in the phosphodiester backbone both 5'- and 3'- to damaged substrates (93). Distinct from the other known [4Fe4S] repair proteins in bacteria, UvrC was found to coordinate an O₂-sensitive [4Fe4S] cluster, causing protein aggregation upon oxidative degradation. Mutation of coordinating cysteines to alanine led to aggregation or severely reduced overexpression, the latter of which has been reported before for MutY (94). Additionally, UvrC in its holo form binds to duplex DNA without lesions, enabling demonstration that UvrC participates in DNA CT chemistry. UvrC shares a DNA-bound midpoint potential with EndoIII, MutY, and DinG. UvrC has been noted in several reports to be unstable *in vitro* and the scarce *in vivo* (~10 copies/cell), so continued

investigation should provide insights as to how chemically and structurally diverse lesions are detected by UvrC in its holo form.

Monitoring Redox Signaling Between Repair Proteins and Repair Pathways

Given the multitude of these clusters, their similarity in redox potential and their diversity in lesions targeted, we became interested in examining how the proteins might cooperate in searching for DNA lesions. To study cooperative, redox communication between [4Fe4S] proteins, a series of *in vitro* and *in vivo* assays were developed to monitor signaling networks. *In vitro*, atomic force microscopy (AFM) has facilitated visualization of [4Fe4S] repair protein distribution on well-matched (WM) DNA versus duplex DNA containing a single base mismatch (MM) (53, 55, 59, 79, 80). Though strands containing a single, engineered C:A mismatch are not native substrates for any of these repair enzymes studied, preferential binding to the 3.8 kb long MM strands, expressed as a binding density ratio of 1.5 (Figure 8), has been seen for all CT-proficient repair proteins. Mixtures of [4Fe4S] proteins from different repair pathways, and, remarkably, mixtures of cluster proteins from distinct organisms also signal cooperatively one to another, localizing to damaged strands.

Two factors have been found to affect the efficiency of the damage search: (i) the CT proficiency of a protein and (ii) the extent to which the protein population is oxidized. Mixing CT-proficient and CT-deficient proteins (*eg.* EndoIII and Y82A) impairs localization to MM strands; the binding density ratio is 1. Protein samples that are 99% oxidized generated anaerobically using DNA electrochemistry also do not redistribute to MM strands, likely due to the >500-fold increase in binding affinity. Redistribution of oxidized EndoIII, however, can be restored with addition of reduced DinG. The same phenomenon was seen in the reciprocal experiment with oxidized DinG and reduced EndoIII. These data underscore that long-range redox signaling between [4Fe4S] enzymes is dependent on the shared DNA-bound redox potential and CT proficiency of the protein. Furthermore, these experiments highlight the ability of the proteins to signal one another over kilobase distances.

Complementary genetics assays were developed using strains of *E. coli* that depend on the repair activity of MutY, DinG, or UvrC for growth. Putative redox signaling networks can be disrupted by genetically knocking out a signaling partner (57, 59, 79). Limited growth in the knocked out strains therefore points to diminished repair activity occurring, owing to limited availability of signaling partners (Figure 9). Complementation plasmids for EndoIII, which include WT enzyme, Y82A, and D138A have been used to monitor how rescue with wild type and EndoIII mutants can restore survival. With this genetic approach, evidence of signaling among BER enzymes, DinG, and UvrC has been found to be necessary for repair activity and growth of cells (57, 59, 79). Rescue with the CT competent but enzymatically deficient D138A but not the CT deficient but enzymatically competent Y82A restores growth in EndoIII knockouts, demonstrating that CT proficiency and not enzymatic activity is needed for redox signaling and efficient repair activity in other pathways.

Diseases and Cancers Related to Mutations in [4Fe4S] Proteins

Mutations linking cancer with compromised repair activity by human [4Fe4S] proteins have been reported (24, 58). Investigations into the redox chemistry of mutant proteins has helped

illuminate how impaired redox signaling capacity could contribute to disease. For example, the CT-deficient EndoIII Y82A mutant corresponds the Y166 of the human homolog, MUTYH. This Y166S mutation has been known to be associated with MAP colorectal cancers (95). Within the context of DNA CT chemistry, a mutation which compromises the CT proficiency of one repair protein could understandably lead to compromised crosstalk of [4Fe4S] repair pathways across the genome.

A novel MUTYH germline variant, C306W, was recently found in a patient with colonic polyposis and a family history of early-onset colon cancer (58). Mutation of C306 does not fully abolish cluster loading or DNA-bound redox activity, but is destabilizing, leading to rapid oxidative degradation of the [4Fe4S] cluster to the [3Fe-4S]⁺ species on a DNA electrode. Degradation of the cluster results in diminished binding to DNA substrates and enzymatic function. The C306W mutant is a powerful example of how cluster degradation disrupts enzymatic activity and redox signaling, emphasizing the critical role of the cluster in preventing the onset of disease. Moreover this degradation occurs only with oxidation, underscoring the important role of the cluster in carrying out redox chemistry.

Mutations in XPD have also been linked to disease, in particular, to three distinct but related disorders with extreme photosensitivity: trichothiodystrophy (TTD), Cockayne syndrome (CS), and xeroderma pigmentosum (XP) (27, 86). Crystal structures of XPD have helped illuminate how common mutations in different domains of XPD lead to specific disorders (96, 97). For example, the L325V mutation (L461 in human XPD), specifically associated with XP and TTD, is CT-deficient relative to the WT enzyme, with diminished ability to distinguish well-matched versus mismatched strands in our AFM assay (55). Another mutation, G34R (G47R in human XPD), is associated with loss of ATP binding and helicase activity. Consistent with this data, the G34R mutant did not exhibit enhanced electronic coupling upon addition of ATP on DNA-modified electrodes (54). Thus, these disease-relevant mutations not only impair enzymatic activity, but also diminish redox signaling capacity.

The study of the redox chemistry and cooperative signaling between disease-relevant mutants has exemplified intimate connections between cluster stability, enzymatic activity, redox activity, and CT proficiency (27). Mutations in other [4Fe4S] proteins may also affect enzymatic or redox signaling activity, and we expect that many heretofore uncharacterized clinically relevant mutations will be linked to compromised redox signaling. The cluster within these proteins thus represents an intriguing new therapeutic target.

Redox-Mediated Catalysis by [4Fe4S] Radical SAM Enzymes

For all of the proteins described thus far, the [4Fe4S] cluster has been involved in redox chemistry but not directly in the enzymatic reaction carried out by the protein. This, however, is not the case for more than 13,500 known radical *S*-adenosyl-L-methionine (SAM) enzymes (98, 99). Radical SAM enzymes employ the tunable, versatile [4Fe4S] cluster cofactor to catalyze essential biochemical reactions, acting on a variety of substrates in multiple metabolic pathways, including repair of UV-induced DNA damage and modification of tRNAs (30, 98, 100–102). These repair proteins, unlike those that carry out redox signaling, contain ferredoxin-like clusters coordinated by three cysteines, which cycle

between the $[4\text{Fe}4\text{S}]^+$ and $[4\text{Fe}4\text{S}]^{2+}$ states during activity. The primary reaction catalyzed by the redox function of the cluster is the generation of a 5'-deoxyadenosyl radical, a powerful, aliphatic oxidant which then catalyzes further biochemical reactions.

One example of repair by a radical SAM enzyme is cleavage of a methylene bridge in a UV-induced DNA lesion by the spore photoproduct lyase (SP lyase), which is responsible for repairing (5R)-5-(α -thyminyloxy)-5,6-dihydrothymidine, or the spore photoproduct, (30). SP lyase has been structurally and biochemically characterized, though chemical properties of the DNA-bound protein are less understood. SP lyase binds a polyanionic substrate that could electrostatically alter the environment and potential of the cluster (103). Comparison of the redox potentials for the $[4\text{Fe}4\text{S}]^{2+/+}$ couple in the presence and absence of a nucleic acid substrate has not yet been explored but will be interesting to consider regarding the chemistry driving catalysis.

VI. $[4\text{Fe}4\text{S}]$ Enzymes in Eukaryotic DNA Replication

Diverse, specialized replication enzymes, many of which contain $[4\text{Fe}4\text{S}]$ clusters, duplicate large eukaryotic genomes with high fidelity (104, 105). DNA primase, B-family polymerases α , δ , and ϵ , the helicase-nuclease Dna2, and the translesion DNA polymerase ζ all contain the $[4\text{Fe}4\text{S}]$ cofactor (62, 63, 106, 107). These multisubunit enzymes, along with the replicative helicase (CMG), processivity factors such as proliferating cell nuclear antigen (PCNA), replication factor C (RFC), and single-stranded binding protein Replication Protein A (RPA), work together to coordinate replication (108–113).

Before polymerases can synthesize new DNA, replication origin sites in the genome must be recognized and licensed through binding of the hexameric origin recognition complex (ORC), followed by Cdc6, Cdt4, and the Mcm2-7 helicase (114–116). Loading of additional proteins, including DNA polymerase ϵ , subsequently forms the pre-initiation complex (113, 114). GINS and Cdc45 associate with Mcm 2-7 and form the active CMG helicase (117–119). The replicative helicase anneals AT-rich DNA at origin sites, beginning bidirectional replication on the two parent strands of genomic DNA. Phosphorylation by cyclin dependent kinase and the Dbf4-dependent kinase spatiotemporally regulates these steps. After annealing and origin firing, polymerases begin DNA synthesis.

DNA Polymerase- α -Primase Begins Replication through Coordinated Binding and Dissociation Events

DNA polymerase- α -primase (pol-prim) is the heterotetrameric complex responsible for synthesizing an RNA-DNA primer which begins DNA synthesis on a template (120). Primase consists of an RNA polymerase subunit p48 and a regulatory subunit p58, and synthesizes an 8-14nt RNA primer on ssDNA (121–123). Polymerase α consists of a catalytic subunit p180 and an auxiliary subunit p70 and synthesizes a ~10-30nt DNA segment downstream of the RNA primer. The C-terminal domain of the primase auxiliary subunit (p58C), and putatively the C-terminal domain of the polymerase α catalytic subunit (p180), coordinate $[4\text{Fe}4\text{S}]$ cofactors (62, 63, 124). To synthesize RNA/DNA primers, primase first binds ssDNA and two nucleotide triphosphates (NTPs). After substrate binding and synthesis of a phosphodiester bond between NTPs, primase is converted to the active

form. Primase then rapidly elongates the primer, and finally truncates synthesis, handing off the template to polymerase α (121–123, 125). After this transfer step, polymerase α binds the RNA/DNA template and deoxynucleotide triphosphates (dNTPs), polymerizing ~10-30 dNTPs downstream of the RNA primer. After this sequence is completed, DNA polymerases ϵ and δ can take over replication.

Primase and polymerase α contain [4Fe4S] clusters but are otherwise structurally and functionally distinct from polymerases δ and ϵ (120, 122). Primase and polymerase α are heterodimers containing catalytic and regulatory subunits. These low-fidelity enzymes lack a proofreading exonuclease domain and have error rates of $\sim 10^{-2}$ (121–123) and $\sim 10^{-4}$ – 10^{-5} (120) respectively, and unlike polymerases ϵ and δ , polymerase α and primase also do not interact with PCNA. Primase [4Fe4S] cluster assembly and fidelity are, moreover, negatively affected by oxidative stress conditions in the cell (126), suggesting cluster sensitivity to the redox environment.

Primase has a Redox Switch

The [4Fe4S] cluster of DNA primase was recently discovered to function as a redox switch, regulating DNA binding and signaling (52). The [4Fe4S] domain of primase, p58C, can bind DNA, independently of the primase enzyme (126, 127). On a DNA-modified electrode, this protein was anaerobically oxidized or reduced using bulk electrolysis. Subsequent CV scans showed that the oxidized [4Fe4S]³⁺ protein was redox-active on DNA, while the reduced [4Fe4S]²⁺ form could not be detected (52). The oxidized protein was bound to the DNA-modified electrode, while the reduced form was only loosely associated. This electrochemically controlled switch is mediated by conserved tyrosines between the cluster and the DNA binding interface (52, 126). Mutation of these tyrosines to phenylalanine or leucine attenuates redox activity on DNA electrodes and compromises primase initiation on ssDNA but not catalytic activity. Moreover, primase truncation is gated by DNA CT *in vitro*; a single base mismatch in a nascent primer abrogates truncation.

In a proposed model of primase-polymerase α handoff (Figure 10), oxidized, tightly bound [4Fe4S]³⁺ primase, coupled into the RNA/DNA duplex, synthesizes the RNA primer. When a reduced [4Fe4S]²⁺ polymerase α cluster contacts the RNA/DNA duplex, polymerase α is oxidized by primase through DNA CT. Our results with human DNA primase indicated that a mismatch formed in the growing DNA/RNA hybrid inhibited this handoff, consistent with the idea that DNA CT facilitates this rapid, long range signaling. Through CT, polymerase α becomes tightly bound in the [4Fe4S]³⁺ form, and primase is reduced to the [4Fe4S]²⁺ form. Primase dissociates from the substrate, allowing polymerase α to bind and synthesize DNA on the template (Figure 10). Redox switching driven by the [4Fe4S] cofactor thus may coordinate these binding and dissociation events.

We recently observed that the redox-driven DNA binding switch is conserved in yeast as well as human primase (128). On DNA electrodes, oxidized [4Fe4S]³⁺ p58C is tightly bound and redox-active, whereas reduced [4Fe4S]²⁺ p58C is loosely associated with DNA and redox-inert in yeast and human systems. Yeast and human redox switches, moreover, are mediated by conserved tyrosines positioned between the p58C DNA binding interface and [4Fe4S] cluster. Remarkably the tyrosines are positioned differently but mediate the same

chemistry in yeast and human primase. Mutations at Y397 in yeast primase moreover cause partial loss of redox signaling and lead to oxidative degradation to a [3Fe4S]⁺ species on DNA. This effect is severe enough to cause lethality in yeast for the p58C Y397L mutation, underscoring the importance of this redox signaling chemistry in essential replication processes.

DNA Polymerases ϵ and δ Divide Labor between Leading and Lagging Strands

Polymerases ϵ and δ are the larger, high-fidelity polymerases responsible for DNA synthesis on the leading and lagging strands, with proofreading 3'→5' exonuclease domains and with mutation rates of $\sim 10^5$ - 10^{-6} and $\sim 10^{-4}$ - 10^{-6} , respectively (120, 129). PCNA binding moreover enhances the intrinsic processivity of both enzymes. The high intrinsic fidelity is necessary for these enzymes, as their products remain in the daughter DNA copy. Pol-prim products, on the other hand, are removed during Okazaki fragment maturation.

The division of replicative labor has been extensively debated and investigated (130–133). Error-prone polymerase studies monitoring ribonucleotide or mispaired base incorporation in an *RnaseH* knockout cell line by error-prone polymerase ϵ or δ mutants has illuminated the distribution of DNA synthesis. A polymerase ϵ variant, *pol2M644G*, caused ribonucleotide incorporation on the leading strand (130, 131). A low-fidelity polymerase δ variant, *pol3L612M*, conversely caused an increase in replication errors, localized on the lagging strand (132). Although polymerase δ can replicate the leading strand templates under certain conditions, polymerase ϵ putatively synthesizes the leading strand and polymerase δ , the lagging strand under normal conditions (133).

The four-subunit polymerase ϵ holoenzyme has a large polymerase subunit, Pol2, which contains two [4Fe4S] clusters. The first cluster, located within the active polymerase domain, is essential for polymerase activity but dispensable for exonuclease activity (134). The second [4Fe4S] cluster is ligated in the Pol2 C-terminal domain, further from the active polymerase site, and is stabilized by coordination with Dpb2 (124). The Dpb2 subunit of polymerase ϵ is associated with the C-terminus of Pol2 and is essential for replisome assembly and checkpoint activation (120). The noncatalytic Dpb3 and Dpb4 subunits likely enhance polymerase ϵ processivity. Characterizing the putative [4Fe4S] clusters in polymerase ϵ will illuminate new roles for DNA-mediated redox signaling in replication in the context of a complex, multisubunit enzyme.

The three-subunit polymerase δ coordinates a [4Fe4S] cluster in the Pol3 subunit catalytic domain. Polymerase δ auxiliary subunit Pol31 associates with Pol3 to stabilize the cluster (124) and the subunit, Pol32 (120, 129). After replication factor C loads PCNA onto DNA, polymerase δ coordinates with PCNA to extend the Okazaki fragments begun by pol-prim (135, 136). PCNA binding greatly enhances polymerase δ processivity, and biochemical evidence suggests that a conformational switch may occur during polymerase δ PCNA binding and activity. (129). Polymerase δ moreover is uniquely capable of strand displacement synthesis (120), consistent with its role in Okazaki fragment maturation, interacting with protein partners like Dna2. DNA polymerase δ is additionally stabilized in the presence of stalled forks during replication stress and may play a role in response to changes in the environment as with oxidative stress (137).

Polymerase δ has been demonstrated electrochemically to be redox-active on DNA, with a midpoint potential near 100 mV vs. NHE in the presence of PCNA (51). With PCNA bound, polymerase δ already binds very tightly to DNA, so it is difficult to consider the cluster oxidation to function as a redox switch for binding. Instead what we observe is that oxidation to the $[4\text{Fe}4\text{S}]^{3+}$ state slows polymerase activity *in vitro*, an effect which can be electrochemically reversed by reducing the protein back to the $[4\text{Fe}4\text{S}]^{2+}$ state. These results inspired a model where PCNA-bound, reduced $[4\text{Fe}4\text{S}]^{2+}$ polymerase δ processively synthesizes DNA. Under oxidizing conditions, the cluster is converted to the $[4\text{Fe}4\text{S}]^{3+}$ form, inducing tighter DNA binding, so tight as to stall activity. Polymerase δ then remains stalled in the oxidized form, consistent with the stalling of polymerase δ found under conditions of oxidative stress. While repair proteins then may be activated with cluster oxidation under conditions of oxidative stress, replication would be inhibited. However, the polymerase can be reduced and restored to the processive form after DNA damage resolution, potentially through long range signaling using DNA CT from repair proteins (Figure 11). Clearly, this signaling needs still to be established, though the electrochemistry and biochemistry show that this long range signaling is possible.

More $[4\text{Fe}4\text{S}]$ Proteins in DNA Processing

In addition to the primary replicative eukaryotic DNA polymerases, several other enzymes have now been discovered to contain $[4\text{Fe}4\text{S}]$ cofactors (29, 107, 124). Dna2 is a $[4\text{Fe}4\text{S}]$ helicase-nuclease enzyme important in double strand break repair, Okazaki fragment maturation, and processing stalled replication forks (138). The cluster in Dna2 is located in the nuclease domain, approximately 10 Å from the bound ssDNA substrate. Dna2 5' \rightarrow 3' endonuclease activity is primarily associated with long flap processing during Okazaki fragment maturation (120). Dna2 also plays a role in preventing regression of stalled replication forks, however, and the enzyme has weak ATP-dependent helicase activity (139, 140). Dna2 function, especially helicase and nuclease coordination, is still unclear; $[4\text{Fe}4\text{S}]$ redox signaling may be important for regulating the multiple cellular roles for Dna2 and its interaction with other $[4\text{Fe}4\text{S}]$ enzymes, such as polymerase δ .

The translesion polymerase ζ also contains a $[4\text{Fe}4\text{S}]$ cluster, coordinated in the Rev3 catalytic subunit (112, 124), which is homologous to other B-family polymerase catalytic subunits. This enzyme also contains a subunit Rev7, and two subunits found in polymerase δ , Pol31 and Pol32, but lacks an exonuclease domain. Interacting with PCNA and many other replication factors, polymerase ζ catalyzes mutagenic polymerase activity in the presence of lesions that stall replication fork progression (112). Finally RNA polymerase II, which synthesizes RNA during transcription, has been demonstrated to contain a $[4\text{Fe}4\text{S}]$ cluster. (29, 112, 141). These proteins may use redox signaling on DNA to coordinate activity in cells, and investigation of their $[4\text{Fe}4\text{S}]$ redox properties will illuminate important biochemical features of the proteins and their pathways.

VII. Summary and Perspectives

Long-range, DNA-mediated redox signaling provides a means to coordinate replication and repair activity across the nucleus. The redox switching driven by a change in cluster

oxidation state regulates DNA association and dissociation with the protein and this redox switch can function rapidly and from a distance without a change in structure of the intervening DNA. This capacity is integral to the DNA CT-driven lesion search in [4Fe4S] repair proteins, in polymerase handoff and in the oxidative stress response. The change in cluster redox potential upon binding the DNA polyanion, the capacity of these DNA-bound proteins to cycle reversibly between [4Fe4S]²⁺ and [4Fe4S]³⁺ redox states, and the ability to promote reactions on DNA from a distance using DNA CT offer powerful chemistry of which to take advantage. DNA CT thus offers a means of rapid communication across the genome among DNA-processing proteins to activate a response, and the [4Fe4S] cluster provides the essential cofactor to carry out this chemistry. As more DNA processing proteins are discovered to contain [4Fe4S] clusters, questions to explore include: (i) which proteins are signaling partners with one another; (ii) how are their redox properties modulating protein activities; and (iii) when protein mutations lead to defects in DNA CT, can we begin to target these defects therapeutically? Certainly, continued investigation of DNA-processing [4Fe4S] enzymes will illuminate the rich and important functional roles of this redox chemistry in the genome.

Acknowledgements.

We are grateful to the NIH (GM126904) for their continued financial support and to our many coworkers and collaborators in elucidating this chemistry.

Literature Cited

1. Beinert H, Holm RH, Munck E. 1997 Iron-sulfur clusters: Nature's modular, multipurpose structures. *Science* 277:653–59 [PubMed: 9235882]
2. Rees DC, Howard JB. 2003 The interface between the biological and inorganic worlds: Iron-sulfur metalloclusters. *Science* 300:929–31 [PubMed: 12738849]
3. Meyer J 2008 Iron-sulfur protein folds, iron-sulfur chemistry, and evolution. *J. Biol. Inorg. Chem* 13:157–70 [PubMed: 17992543]
4. Dey A, Jenney FE, Adams MWW, Babini E, Takahashi Y, et al. 2007 Solvent tuning of electrochemical potentials in the active sites of HiPIP versus ferredoxin. *Science* 318:1464–68 [PubMed: 18048692]
5. Ha Y, Arnold AR, Nuñez NN, Bartels PL, Zhou A, et al. 2017 Sulfur K-Edge XAS Studies of the Effect of DNA Binding on the [Fe4S4] Site in EndoIII and MutY. *J. Am. Chem. Soc* 139:11434–42 [PubMed: 28715891]
6. Bertini I, Gray HB, Lippard SJ, Valentine JS. 1994 *Bioinorganic Chemistry University Books*
7. Mortenson LE, Valentine RC, Carnahan JE. 1962 An electron transport factor from *Clostridium pasteurianum*. *Biochem. Biophys. Res. Commun* 7:448–52 [PubMed: 14476372]
8. Sands RH, Beinert H. 1960 Studies on mitochondria and submitochondrial particles by paramagnetic resonance (EPR) spectroscopy. *Biochem. Biophys. Res. Commun* 3:47–52
9. Arnon DI, Whatley FR, Allen MB. 1957 Triphosphopyridine nucleotide as a catalyst of photosynthetic phosphorylation. *Nature* 180:182–85 [PubMed: 13451670]
10. Gray HB, Winkler JR. 2010 Electron flow through metalloproteins. *Biochim. Biophys. Acta - Bioenerg.* 1797:1563–72
11. Winkler JR, Gray HB. 2014 Electron Flow through Metalloproteins. *Chem. Rev* 114:3369–80 [PubMed: 24279515]
12. Cunningham RP, Asahara H, Bank JF, Scholes CP, Salerno JC, et al. 1989 Endonuclease III Is an Iron-Sulfur Protein. *Biochemistry* 28:4450–55 [PubMed: 2548577]

13. Rouault TA. 2015 Mammalian iron-sulphur proteins: novel insights into biogenesis and function. *Nat Rev Mol Cell Biol* 16:45–55 [PubMed: 25425402]
14. Johnson DC, Dean DR, Smith AD, Johnson MK. 2005 Structure, Function, and Formation of Biological Iron-Sulfur Clusters. *Annu. Rev. Biochem* 74:247–81 [PubMed: 15952888]
15. Braymer JJ, Lill R. 2017 Iron-sulfur cluster biogenesis and trafficking in mitochondria. *J. Biol. Chem* 292:12754–63 [PubMed: 28615445]
16. Paul VD, Lill R. 2015 Biogenesis of cytosolic and nuclear iron-sulfur proteins and their role in genome stability. *Biochim. Biophys. Acta - Mol. Cell Res* 1853:1528–39
17. Rouault TA, Maio N. 2017 Biogenesis and functions of mammalian iron-sulfur proteins in the regulation of iron homeostasis and pivotal metabolic pathways. *J. Biol. Chem* 292:12744–53 [PubMed: 28615439]
18. Rubio LM, Ludden PW. 2008 Biosynthesis of the Cofactor of Nitrogenase. *Annu. Rev. Microbiol* 62:93–111 [PubMed: 18429691]
19. Wayne Outten F 2015 Recent advances in the Suf Fe-S cluster biogenesis pathway: Beyond the Proteobacteria. *Biochim. Biophys. Acta - Mol. Cell Res* 1853:1464–69
20. Ezraty B, Vergnes A, Banzhaf M, Duverger Y, Huguenot A, et al. 2013 Fe-S cluster biosynthesis controls uptake of aminoglycosides in a ROS-less death pathway. *Science* 340:1583–87 [PubMed: 23812717]
21. White MF, Dillingham MS. 2012 Iron-sulphur clusters in nucleic acid processing enzymes. *Curr. Opin. Struct. Biol* 22:94–100 [PubMed: 22169085]
22. Guan Y, Manuel RC, Arvai AS, Parikh SS, Mol CD, et al. 1998 MutY catalytic core, mutant and bound adenine structures define specificity for DNA repair enzyme superfamily. *Nat. Struct. Biol* 5:1058–64 [PubMed: 9846876]
23. Hinks JA, Evans MCW, De Miguel Y, Sartori AA, Jiricny J, Pearl LH. 2002 An iron-sulfur cluster in the Family 4 uracil-DNA glycosylases. *J. Biol. Chem* 277:16936–40 [PubMed: 11877410]
24. Bartels PL, O'Brien E, Barton JK. 2017 DNA signaling by iron-sulfur cluster proteins In *Biochemistry, Biosynthesis and Human Diseases: Biochemistry, Biosynthesis, and Human Diseases*, ed TA Rouault. 2:405–23. Berlin, Boston: De Gruyter
25. Zhang F, Scheerer P, Oberpichler I, Lamparter T, Krauss N. 2013 Crystal structure of a prokaryotic (6-4) photolyase with an Fe-S cluster and a 6,7-dimethyl-8-ribityllumazine antenna chromophore. *PNAS* 110:7217–22 [PubMed: 23589886]
26. Zhang J, Kasciukovic T, White MF. 2012 The CRISPR Associated Protein Cas4 Is a 5' to 3' DNA Exonuclease with an Iron-Sulfur Cluster. *PLoS One*. 7:e47232 [PubMed: 23056615]
27. Fuss JO, Tsai CL, Ishida JP, Tainer JA. 2015 Emerging critical roles of Fe-S clusters in DNA replication and repair. *Biochim. Biophys. Acta - Mol. Cell Res* 1853:1253–71
28. Silva RMB, Grodick MA, Barton JK. 2018. in preparation
29. Hirata A, Klein BJ, Murakami KS. 2008 The X-ray crystal structure of RNA polymerase from Archaea. *Nature* 451:851–54 [PubMed: 18235446]
30. Benjdia A, Heil K, Barends TRM, Carell T, Schlichting I. 2012 Structural insights into recognition and repair of UV-DNA damage by Spore Photoproduct Lyase, a radical SAM enzyme. *Nucleic Acids Res* 40:9308–18 [PubMed: 22761404]
31. Rouault TA. 2015 Iron-sulfur proteins hiding in plain sight. *Nat. Chem. Biol* 11:442–45 [PubMed: 26083061]
32. Boal AK, Yavin E, Lukianova OA, O'Shea VL, David SS, Barton JK. 2005 DNA-bound redox activity of DNA repair glycosylases containing [4Fe-4S] clusters. *Biochemistry* 44:8397–8407 [PubMed: 15938629]
33. Fu W, O'Handley S, Cunningham RP, Johnson MK. 1992 The role of the iron-sulfur cluster in Escherichia coli endonuclease III. A resonance Raman study. *J. Biol. Chem* 267:16135–37 [PubMed: 1644800]
34. Thayer MM, Ahern H, Xing D, Cunningham RP, Tainer J a. 1995 Novel DNA binding motifs in the DNA repair enzyme endonuclease III crystal structure. *EMBO J*. 14:4108–20 [PubMed: 7664751]

35. Muty G, Porello SL, Cannon MJ, David SS. 1998 A Substrate Recognition Role for the [4Fe-4S] 2 + Cluster of the DNA Repair. *Society*. 2960:6465–75
36. Imlay JA. 2013 The molecular mechanisms and physiological consequences of oxidative stress: lessons from a model bacterium. *Nat. Rev. Microbiol* 11:443–54 [PubMed: 23712352]
37. Genereux JC, Barton JK. 2010 Mechanisms for DNA charge transport. *Chem. Rev* 110:1642–62 [PubMed: 20214403]
38. Eley DD, Spivey DI. 1962 Semiconductivity of organic substances. IX. Nucleic acid in the dry state. *Trans. Faraday Soc* 58:411–15
39. Murphy CJ, Arkin MR, Jenkins Y, Ghatlia ND, Bossmann SH, et al. 1993 Long-range photoinduced electron transfer through a DNA helix. *Science* 262:1025–29 [PubMed: 7802858]
40. Kelley SO, Barton JK. 1999 Electron transfer between bases in double helical DNA. *Science* 283:375–81 [PubMed: 9888851]
41. Nunez ME, Hall DB, Barton JK. 1999 Long-range oxidative damage to DNA: effects of distance and sequence. *Chem. Biol* 6:85–97 [PubMed: 10021416]
42. O'Neill MA, Becker HC, Wan C, Barton JK, Zewail AH. 2003 Ultrafast Dynamics in DNA-Mediated Electron Transfer: Base Gating and the Role of Temperature. *Angew. Chemie - Int. Ed* 42:5896–5900
43. Giese B, Graber M, Cordes M. 2008 Electron transfer in peptides and proteins. *Curr. Opin. Chem. Biol* 12:755–59 [PubMed: 18804174]
44. Phillips R, Kondev J, Theriot J. 2008 *Physical Biology of the Cell* London: Garland Science, Taylor and Francis Group 1st ed.
45. Rajski SR, Barton JK. 2001 How different DNA-binding proteins affect long-range oxidative damage to DNA. *Biochemistry* 40:5556–64 [PubMed: 11331021]
46. Boon EM, Salas JE, Barton JK. 2002 An electrical probe of protein-DNA interactions on DNA-modified surfaces. *Nat. Biotechnol* 20:282–86 [PubMed: 11875430]
47. Nunez ME, Noyes KT, Barton JK. 2002 Oxidative charge transport through DNA in nucleosome core particles. *Chem. Biol* 9:403–15 [PubMed: 11983330]
48. Slinker JD, Muren NB, Renfrew SE, Barton JK. 2011 DNA charge transport over 34 nm. *Nat. Chem* 3:228–33 [PubMed: 21336329]
49. Slinker JD, Muren NB, Gorodetsky AA, Barton JK. 2010 Multiplexed DNA-modified electrodes. *J. Am. Chem. Soc* 132:2769–74 [PubMed: 20131780]
50. Pheaney CG, Arnold AR, Grodick MA, Barton JK. 2013 Multiplexed electrochemistry of DNA-bound metalloproteins. *J. Am. Chem. Soc* 135:11869–78 [PubMed: 23899026]
51. Bartels PL, Stodola JL, Burgers PMJ, Barton JK. 2017 A Redox Role for the [4Fe4S] Cluster of Yeast DNA Polymerase δ . *J. Am. Chem. Soc* 139:18339–48 [PubMed: 29166001]
52. O'Brien E, Holt ME, Thompson MK, Salay LE, Ehlinger AC, et al. 2017 The [4Fe4S] cluster of human DNA primase functions as a redox switch using DNA charge transport. *Science* 355:eaag1789 [PubMed: 28232525]
53. Tse ECM, Zwang TJ, Barton JK. 2017 The Oxidation State of [4Fe4S] Clusters Modulates the DNA-Binding Affinity of DNA Repair Proteins. *J. Am. Chem. Soc* 139:12784–92 [PubMed: 28817778]
54. Mui TP, Fuss JO, Ishida JP, Tainer JA, Barton JK. 2011 ATP-stimulated, DNA-mediated redox signaling by XPD, a DNA repair and transcription helicase. *J. Am. Chem. Soc* 133:16378–81 [PubMed: 21939244]
55. Sontz PA, Mui TP, Fuss JO, Tainer JA, Barton JK. 2012 DNA charge transport as a first step in coordinating the detection of lesions by repair proteins. *PNAS* 109:1856–61 [PubMed: 22308447]
56. Ekanger L, Oyala PH, Moradian A, Sweredoski MJ, Barton JK. 2018. Submitted
57. Zhou A, Ph.D thesis, California Institute of Technology, 2018.
58. McDonnell KJ, Chemler JA, Bartels PL, O'Brien E, Marvin ML, et al. A human MUTYH variant linking colonic polyposis to redox degradation of the [4Fe4S]₂⁺ cluster. *Nat. Chem*
59. Grodick MA, Segal HM, Zwang TJ, Barton JK. 2014 DNA-mediated signaling by proteins with 4Fe-4S clusters is necessary for genomic integrity. *J. Am. Chem. Soc* 136:6470–78 [PubMed: 24738733]

60. Gorodetsky Alon A., Amie K. Boal A, Barton JK. 2006 Direct Electrochemistry of Endonuclease III in the Presence and Absence of DNA. *J. Am. Chem. Soc* 128:12082–83 [PubMed: 16967954]
61. Bartels PL, Zhou A, Arnold AR, Nunez NN, Crespilho FN, et al. 2017 Electrochemistry of the [4Fe4S] Cluster in Base Excision Repair Proteins: Tuning the Redox Potential with DNA. *Langmuir* 33:2523–30 [PubMed: 28219007]
62. Klinge S, Hirst J, Maman JD, Krude T, Pellegrini L. 2007 An iron-sulfur domain of the eukaryotic primase is essential for RNA primer synthesis. *Nat. Struct. Mol. Biol* 14:875–77 [PubMed: 17704817]
63. Weiner BE, Huang H, Dattilo BM, Nilges MJ, Fanning E, Chazin WJ. 2007 An iron-sulfur cluster in the C-terminal domain of the p58 subunit of human DNA primase. *J. Biol. Chem* 282:33444–51 [PubMed: 17893144]
64. Ren B, Duan X, Ding H. 2009 Redox control of the DNA damage-inducible protein DinG helicase activity via its iron-sulfur cluster. *J. Biol. Chem* 284:4829 [PubMed: 19074432]
65. Rudolf J, Makranton V, Inglede WJ, Stark MJR, White MF. 2006 The DNA Repair Helicases XPD and FancJ Have Essential Iron-Sulfur Domains. *Mol. Cell*. 23:801–8 [PubMed: 16973432]
66. Yavin E, Boal AK, Stemp EDA, Boon EM, Livingston AL, et al. 2005 Protein-DNA charge transport: Redox activation of a DNA repair protein by guanine radical. *PNAS* 102:3546–51 [PubMed: 15738421]
67. Ciccia A, Elledge SJ. 2010 The DNA Damage Response: Making It Safe to Play with Knives. *Mol. Cell* 40:179–204 [PubMed: 20965415]
68. Marsden CG, Dragon JA, Wallace SS, Sweasy JB. 2017 Base Excision Repair Variants in Cancer. *Methods Enzymol* 591:119–57 [PubMed: 28645367]
69. Gorman J, Greene EC. 2008 Visualizing one-dimensional diffusion of proteins along DNA. *Nat. Struct. Mol. Biol* 15:768–74 [PubMed: 18679428]
70. Christmann M, Kaina B. 2013 Transcriptional regulation of human DNA repair genes following genotoxic stress: Trigger mechanisms, inducible responses and genotoxic adaptation. *Nucleic Acids Res* 41:8403–20 [PubMed: 23892398]
71. Boal AK, Barton JK. 2005 Electrochemical detection of lesions in DNA. *Bioconjug. Chem* 16:312–21 [PubMed: 15769084]
72. Hall DB, Holmlin RE, Barton JK. 1996 Oxidative DNA damage through long-range electron transfer. *Nature* 382:731–35 [PubMed: 8751447]
73. David SS, Williams SD. 1998 Chemistry of Glycosylases and Endonucleases Involved in Base-Excision Repair. *Chem. Rev* 98:1221–62 [PubMed: 11848931]
74. David SS, O'Shea VL, Kundu S. 2007 Base-excision repair of oxidative DNA damage. *Nature*. 447:941–50 [PubMed: 17581577]
75. Fromme JC, Verdine GL. 2003 Structure of a trapped endonuclease III-DNA covalent intermediate. *EMBO J*. 22:3461–71 [PubMed: 12840008]
76. Engstrom LM, Partington OA, David SS. 2012 An iron-sulfur cluster loop motif in the archaeoglobus fulgidus uracil-DNA glycosylase mediates efficient uracil recognition and removal. *Biochemistry* 51:5187–97 [PubMed: 22646210]
77. Lukianova OA, David SS. 2005 A role for iron-sulfur clusters in DNA repair. *9(2):145–51*
78. Weren RDA, Ligtenberg MJL, Geurts van Kessel A, De Voer RM, Hoogerbrugge N, Kuiper RP. 2018 NTHL1 and MUTYH polyposis syndromes: two sides of the same coin? *J. Pathol* 244:135–42 [PubMed: 29105096]
79. Boal AK, Genereux JC, Sontz PA, Gralnick JA, Newman DK, Barton JK. 2009 Redox signaling between DNA repair proteins for efficient lesion detection. *PNAS* 106: 15237–15242 [PubMed: 19720997]
80. Romano CA, Sontz PA, Barton JK. 2011 Mutants of the base excision repair glycosylase, endonuclease III: DNA charge transport as a first step in lesion detection. *Biochemistry* 50:6133–45 [PubMed: 21651304]
81. Wu Y, Brosh RM. 2012 DNA helicase and helicase-nuclease enzymes with a conserved iron-sulfur cluster. *Nucleic Acids Res* 40:4247–60 [PubMed: 22287629]

82. Brosh RM. 2013 DNA helicases involved in DNA repair and their roles in cancer. *Nat. Rev. Cancer* 13:542–58 [PubMed: 23842644]
83. Vannier JB, Sarek G, Boulton SJ. 2014 RTEL1: Functions of a disease-associated helicase. *Trends Cell Biol* 24:416–25 [PubMed: 24582487]
84. Voloshin ON, Camerini-Otero RD. 2007 The DinG protein from *Escherichia coli* is a structure-specific helicase. *J. Biol. Chem* 282:18437–47 [PubMed: 17416902]
85. Brown LT, Sutera VA, Zhou S, Weitzel CS, Cheng Y, Lovett ST. 2015 Connecting Replication and Repair: YoaA, a Helicase-Related Protein, Promotes Azidothymidine Tolerance through Association with Chi, an Accessory Clamp Loader Protein. *PLoS Genet* 11:e1005651 [PubMed: 26544712]
86. Houten B Van, Kuper J, Kisker C. 2016 Role of XPD in cellular functions: To TFIIH and beyond. *DNA Repair* 44:136–42 [PubMed: 27262611]
87. Brosh RM, Cantor SB. 2014 Molecular and cellular functions of the FANCD1 DNA helicase defective in cancer and in Fanconi anemia. *Front. Genet* 5:372 [PubMed: 25374583]
88. Grodick MA, Muren NB, Barton JK. 2015 DNA charge transport within the cell. *Biochemistry* 54:962–73 [PubMed: 25606780]
89. Guo M, Hundseth K, Ding H, Vidhyasagar V, Inoue A, et al. 2015 A distinct triplex DNA unwinding activity of ChlR1 helicase. *J. Biol. Chem* 290:5174–89 [PubMed: 25561740]
90. Yeeles JTP, Cammack R, Dillingham MS. 2009 An iron-sulfur cluster is essential for the binding of broken DNA by AddAB-type helicase-nucleases. *J. Biol. Chem* 284:7746–55 [PubMed: 19129187]
91. Lenhart JS, Schroeder JW, Walsh BW, Simmons LA. 2012 DNA Repair and Genome Maintenance in *Bacillus subtilis*. *Microbiol. Mol. Biol. Rev* 76:530–64 [PubMed: 22933559]
92. Saikrishnan K, Yeeles JT, Gilhooly NS, Krajewski WW, Dillingham MS, Wigley DB. 2012 Insights into Chi recognition from the structure of an AddAB-type helicase-nuclease complex. *EMBO J.* 31:1568–78 [PubMed: 22307084]
93. Kisker C, Kuper J, Houten B Van, Houten B Van. 2013 Prokaryotic nucleotide excision repair. *Cold Spring Harb. Perspect. Biol* 5:1–18
94. Golinelli MP, Chmiel NH, David SS. 1999 Site-directed mutagenesis of the cysteine ligands to the [4Fe-4S] cluster of *Escherichia coli* MutY. *Biochemistry.* 38:6997–7007 [PubMed: 10353811]
95. Cheadle JP, Sampson JR. 2007 MUTYH-associated polyposis-From defect in base excision repair to clinical genetic testing. *DNA Repair* 6:274–79 [PubMed: 17161978]
96. Fan L, Fuss JO, Cheng QJ, Arvai AS, Hammel M, et al. 2008 XPD Helicase Structures and Activities: Insights into the Cancer and Aging Phenotypes from XPD Mutations. *Cell* 133:789–800 [PubMed: 18510924]
97. Wolski SC, Kuper J, Hanzelmann P, Truglio JJ, Croteau DL, et al. 2008 Crystal structure of the FeS cluster-containing nucleotide excision repair helicase XPD. *PLoS Biol* 6:1332–42
98. Lanz ND, Booker SJ. 2015 Auxiliary iron-sulfur cofactors in radical SAM enzymes. *Biochim. Biophys. Acta - Mol. Cell Res* 1853:1316–34
99. Maiocco SJ, Grove TL, Booker SJ, Elliott SJ. 2015 Electrochemical Resolution of the [4Fe-4S] Centers of the AdoMet Radical Enzyme BtrN: Evidence of Proton Coupling and an Unusual, Low-Potential Auxiliary Cluster. *J. Am. Chem. Soc* 137:8664–67 [PubMed: 26088836]
100. Marquet A, Florentin D, Ploux O, Bui BTS. 1998 In vivo formation of C-S bonds in biotin. An example of radical chemistry under reducing conditions. *J. Phys. Org. Chem* 11:529–35
101. Anton BP, Saleh L, Benner JS, Raleigh EA, Kasif S, Roberts RJ. 2008 RimO, a MiaB-like enzyme, methylthiolates the universally conserved Asp88 residue of ribosomal protein S12 in *Escherichia coli*. *PNAS* 105:1826–31 [PubMed: 18252828]
102. Schwalm EL, Grove TL, Booker SJ, Boal AK. 2016 Crystallographic capture of a radical S-adenosylmethionine enzyme in the act of modifying tRNA. *Science* 352:309–12 [PubMed: 27081063]
103. Kneutinger AC, Heil K, Kashiwazaki G, Carell T. 2013 The radical SAM enzyme spore photoproduct lyase employs a tyrosyl radical for DNA repair. *Chem. Commun* 49:722–24

104. Moran U, Phillips R, Milo R. 2010 SnapShot: Key numbers in biology. *Cell* 141:1262 [PubMed: 20603006]
105. Ganai RA, Johansson E. 2016 DNA Replication - a Matter of Fidelity. *Mol. Cell* 62:745–55 [PubMed: 27259205]
106. Netz DJA, Stith CM, Stumpfig M, Köpf G, Vogel D, et al. 2011 Eukaryotic DNA polymerases require an iron-sulfur cluster for the formation of active complexes. *Nat. Chem. Biol* 8:125–32 [PubMed: 22119860]
107. Pokharel S, Campbell JL. 2012 Cross talk between the nuclease and helicase activities of Dna2: Role of an essential iron-sulfur cluster domain. *Nucleic Acids Res* 40:7821–30 [PubMed: 22684504]
108. Baranovskiy AG, Babayeva ND, Zhang Y, Gu J, Suwa Y, et al. 2016 Mechanism of Concerted RNA-DNA Primer Synthesis by the Human Primosome. *J. Biol. Chem* 291:10006–20 [PubMed: 26975377]
109. Johansson E, Majka J, Burgers PMJ. 2001 Structure of DNA Polymerase δ from *Saccharomyces cerevisiae*. *J. Biol. Chem* 276:43824–28 [PubMed: 11568188]
110. Chilkova O, Jonsson B-H, Johansson E. 2003 The Quaternary Structure of DNA Polymerase ϵ from *Saccharomyces cerevisiae*. *J. Biol. Chem* 278:14082–86 [PubMed: 12571237]
111. Nelson JR, Lawrence CW, Hinkle DC. 1996 Thymine-thymine dimer bypass by yeast DNA polymerase ζ . *Science* 272:1646–49 [PubMed: 8658138]
112. Makarova AV, Burgers PM. 2015 Eukaryotic DNA polymerase ζ . *DNA Repair* 29:47–55 [PubMed: 25737057]
113. Yeeles JTP, Deegan TD, Janska A, Early A, Diffley JFX. 2015 Regulated eukaryotic DNA replication origin firing with purified proteins. *Nature* 519:431–35 [PubMed: 25739503]
114. Fragkos M, Ganier O, Coulombe P, Mechali M. 2015 DNA replication origin activation in space and time. *16(6):360–74*
115. Iyer LM, Leippe DD, Koonin EV, Aravind L. 2004 Evolutionary history and higher order classification of AAA+ ATPases. *J. Struct. Biol* 146:11–31 [PubMed: 15037234]
116. Duncker BP, Chesnokov IN, McConkey BJ. 2009 The origin recognition complex protein family. *Genome Biol* 10:214 [PubMed: 19344485]
117. Moyer SE, Lewis PW, Botchan MR. 2006 Isolation of the Cdc45/Mcm2-7/GINS (CMG) complex, a candidate for the eukaryotic DNA replication fork helicase. *PNAS*. 103:10236–41 [PubMed: 16798881]
118. Pacek M, Tutter AV., Kubota Y, Takisawa H, Walter JC. 2006 Localization of MCM2-7, Cdc45, and GINS to the site of DNA unwinding during eukaryotic DNA replication. *Mol. Cell* 21:581–87 [PubMed: 16483939]
119. Labib K, Gambus A. 2007 A key role for the GINS complex at DNA replication forks. *Trends Cell Biol* 17:271–78 [PubMed: 17467990]
120. Burgers PMJ, Kunkel TA. 2017 Eukaryotic DNA Replication Fork. *Annu. Rev. Biochem* 86:417–38 [PubMed: 28301743]
121. Arezi B, Kuchta RD. 2000 Eukaryotic DNA primase. *Trends Biochem. Sci* 25:572–76 [PubMed: 11084371]
122. Kuchta RD, Stengel G. 2010 Mechanism and evolution of DNA primases. *Biochim. Biophys. Acta - Proteins Proteomics*. 1804:1180–89
123. Frick DN, Richardson CC. 2001 DNA primases. *Annu. Rev. Biochem* 70:39–80 [PubMed: 11395402]
124. Netz DJA, Mascarenhas J, Stehling O, Pierik AJ, Lill R. 2014 Maturation of cytosolic and nuclear iron-sulfur proteins. *Trends Cell Biol* 24:303–12 [PubMed: 24314740]
125. Núñez-Ramírez R, Klinge S, Sauguet L, Melero R, Recuero-Checa MA, et al. 2011 Flexible tethering of primase and DNA Pol α in the eukaryotic primosome. *Nucleic Acids Res* 39:8187–99 [PubMed: 21715379]
126. Liu L, Huang M. 2015 Essential role of the iron-sulfur cluster binding domain of the primase regulatory subunit Pri2 in DNA replication initiation. *Protein Cell* 6:194–210 [PubMed: 25645023]

127. Vaithiyalingam S, Warren EM, Eichman BF, Chazin WJ. 2010 Insights into eukaryotic DNA priming from the structure and functional interactions of the 4Fe-4S cluster domain of human DNA primase. *PNAS* 107:13684–89 [PubMed: 20643958]
128. O'Brien E, Salay LE., Epum EA, Friedman KL, Chazin WJ, Barton JK. 2018. Submitted
129. Garg P, Burgers PMJ. 2005 DNA polymerases that propagate the eukaryotic DNA replication fork. *Crit. Rev. Biochem. Mol. Biol* 40:115–28 [PubMed: 15814431]
130. McElhinny SAN, Kumar D, Clark AB, Watt DL, Watts BE, et al. 2010 Genome instability due to ribonucleotide incorporation into DNA. *Nat. Chem. Biol* 6:774–81 [PubMed: 20729855]
131. Lujan SA, Williams JS, Clausen AR, Clark AB, Kunkel TA. 2013 Ribonucleotides are signals for mismatch repair of leading-strand replication errors. *Mol. Cell* 50:437–43 [PubMed: 23603118]
132. McElhinny SAN, Stith CM, Burgers PMJ, Kunkel TA. 2007 Inefficient proofreading and biased error rates during inaccurate DNA synthesis by a mutant derivative of *Saccharomyces cerevisiae* DNA polymerase. *J. Biol. Chem* 282:2324–32 [PubMed: 17121822]
133. Johnson RE, Klassen R, Prakash L, Prakash S. 2015 A Major Role of DNA Polymerase δ in Replication of Both the Leading and Lagging DNA Strands. *Mol. Cell* 59:163–75 [PubMed: 26145172]
134. Jain R, Vanamee ES, Dzikovski BG, Buku A, Johnson RE, et al. 2014 An iron-sulfur cluster in the polymerase domain of yeast DNA polymerase ϵ . *J. Mol. Biol* 426:301–8 [PubMed: 24144619]
135. Tsurimoto T, Stillman B. 1991 Replication factors required for SV40 DNA replication in vitro. I. DNA structure-specific recognition of a primer-template junction by eukaryotic DNA polymerases and their accessory proteins. *J. Biol. Chem* 266:1950–60 [PubMed: 1671045]
136. Yuzhakov A, Kelman Z, Hurwitz J, O'Donnell M. 1999 Multiple competition reactions for RPA order the assembly of the DNA polymerase delta holoenzyme. *EMBO J.* 18:6189–99 [PubMed: 10545128]
137. De Piccoli G, Katou Y, Itoh T, Nakato R, Shirahige K, Labib K. 2012 Replisome Stability at Defective DNA Replication Forks Is Independent of S Phase Checkpoint Kinases. *Mol. Cell* 45:696–704 [PubMed: 22325992]
138. Zhou C, Pourmal S, Pavletich NP. 2015 Dna2 nuclease-helicase structure, mechanism and regulation by Rpa. *Elife* 4:e09832 [PubMed: 26491943]
139. Hu J, Sun L, Shen F, Chen Y, Hua Y, et al. 2012 The intra-S phase checkpoint targets Dna2 to prevent stalled replication forks from reversing. *Cell* 149:1221–32 [PubMed: 22682245]
140. Budd ME, Choe WC, Campbell JL. 2000 The nuclease activity of the yeast Dna2 protein, which is related to the RecB-like nucleases, is essential in vivo. *J. Biol. Chem* 275:16518–29 [PubMed: 10748138]
141. Jennings ME, Lessner FH, Karr EA, Lessner DJ. 2017 The [4Fe-4S] clusters of Rpo3 are key determinants in the post Rpo3/Rpo11 heterodimer formation of RNA polymerase in *Methanosarcina acetivorans*. *Microbiologyopen*. 6:e00399

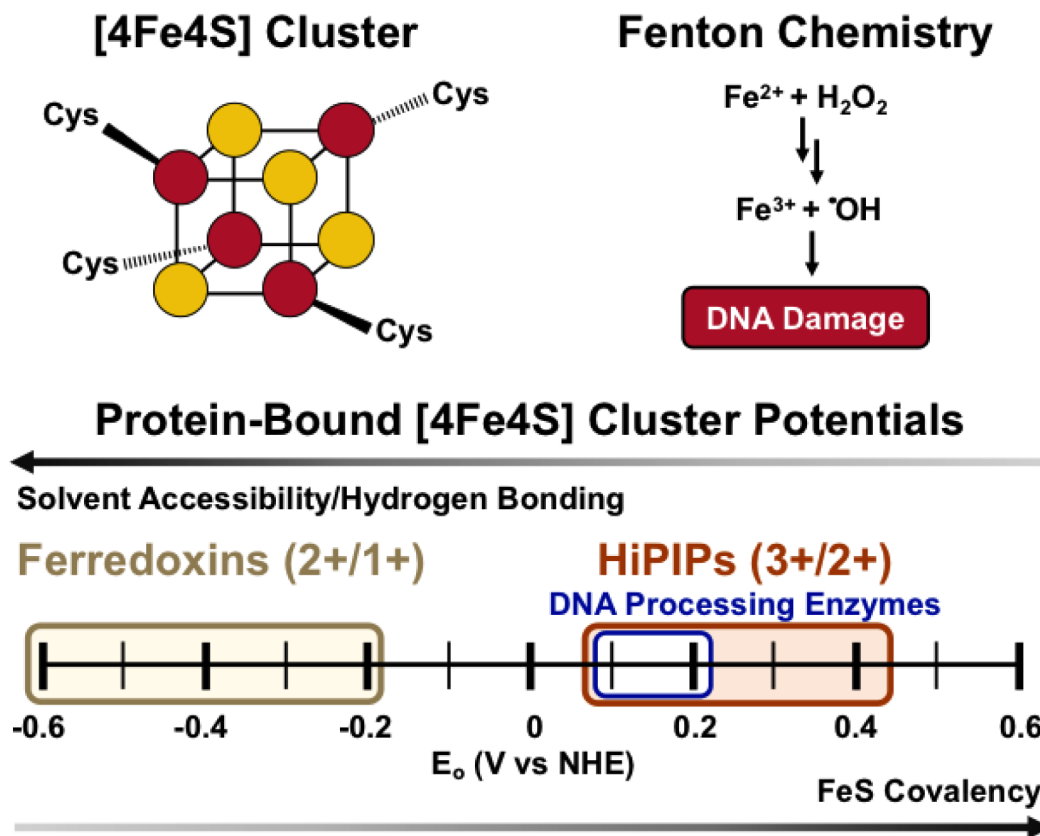
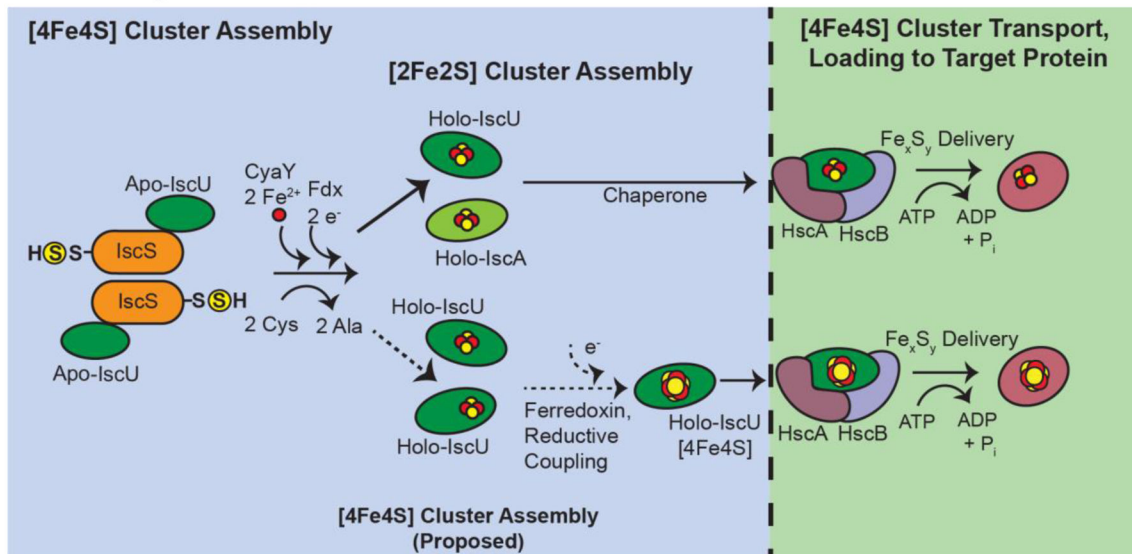


Figure 1. [4Fe₄S] Clusters.

(Above, left) Schematic of the cubane [4Fe₄S] cluster, with Fe in red and S in yellow. (Above, right) Cofactors containing iron can react with cellular oxidants leading to Fenton chemistry and DNA damage by the hydroxyl radical. (Below) The potential of the [4Fe₄S] cluster cofactor is tunable over a wide range of physiological redox potential values. Ferredoxins access the [4Fe₄S]^{2+/1+} couple, upon reduction from the resting [4Fe₄S]²⁺ state. (yellow). High potential iron proteins (HiPIPs) access the [4Fe₄S]^{3+/2+} couple upon oxidation to the [4Fe₄S]³⁺ state from the resting [4Fe₄S]²⁺ state (red). DNA-processing enzymes with [4Fe₄S] cofactors have DNA-bound redox potentials which fall within the HiPIP [4Fe₄S]^{3+/2+} potential range, at approximately ~65-150mV vs. NHE (blue). The solvent accessibility and hydrogen bonding/electrostatic environment of the cluster all contribute to tuning the redox potential of the cofactor (4,5).

Prokaryotes



Eukaryotes

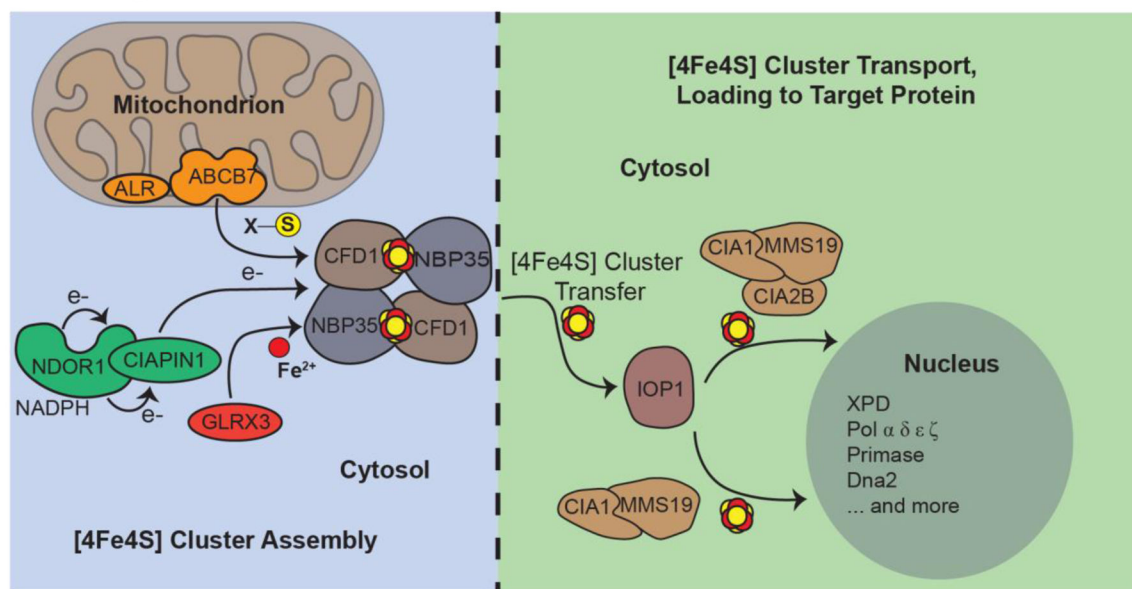


Figure 2. [4Fe4S] cluster biogenesis and loading into prokaryotic (above) and eukaryotic (below) target proteins.

Scaffold proteins, together with cysteine desulfurases and ferrous iron sources, assemble the cluster and bind chaperone machinery to then transport the cofactor first to machinery responsible for cluster delivery, then finally to target proteins. This process is not identical in bacteria and eukaryotes. However each process requires the concerted action of several specialized proteins and requires significant metabolic expense for the cell (13-19).

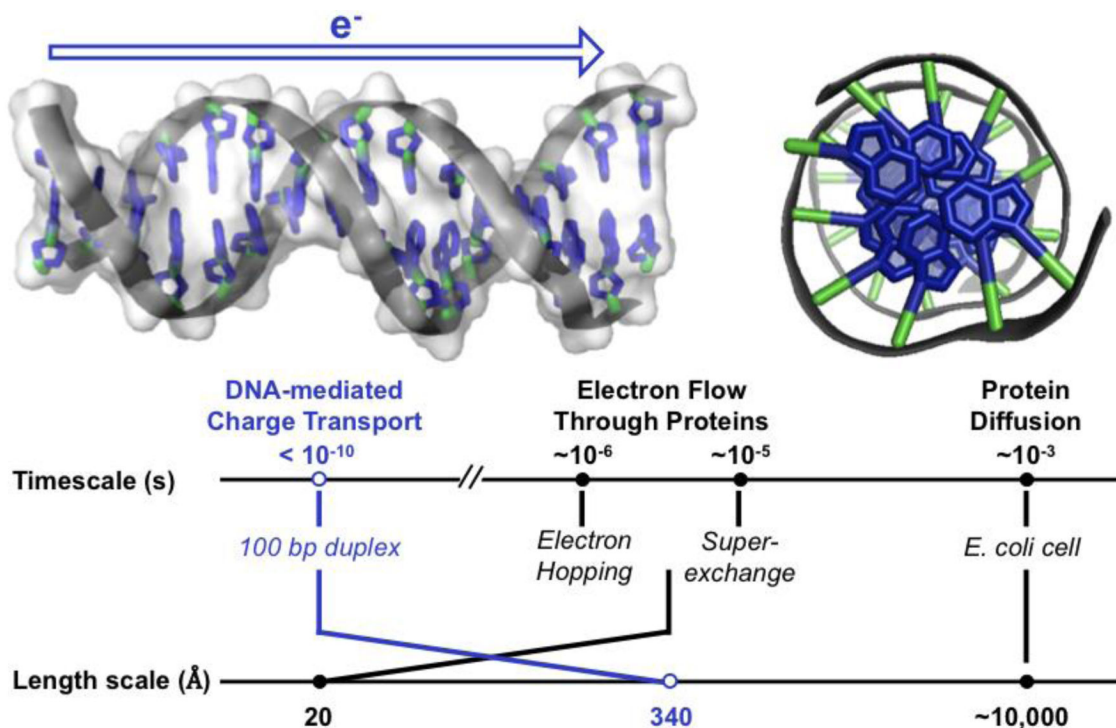


Figure 3. The structure of DNA facilitates long-range, rapid electron transfer. (Top, left) Side view of DNA. The aromatic bases at the center of the DNA helix are oriented so that the π orbitals of adjacent bases overlap with one another in the duplex. This structural property suggests that charge could pass through the π -stacked base pairs of DNA. (Top, right) View down the helical axis of aromatic base pairs (blue) stacked in 3.4 Å layers at the center of DNA. (Bottom) Time scale and length scale of various electron transfer pathways through biomolecules (10, 11,41,43). PDB ID **3BSE**.

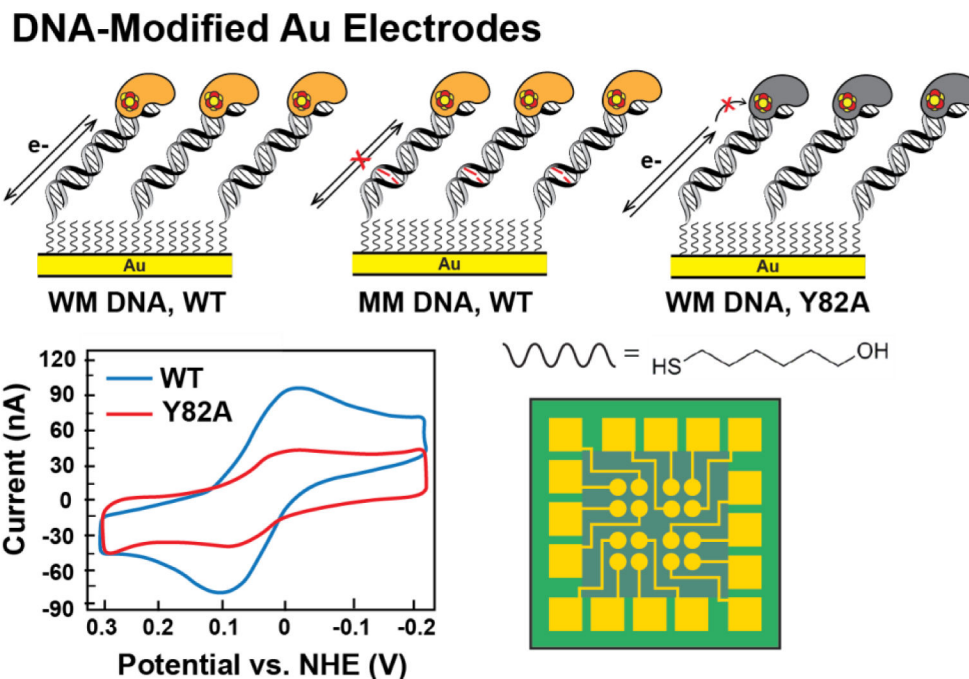


Figure 4. Measuring the redox potential of DNA-bound [4Fe4S] enzymes.

(Top) DNA electrochemistry on Au electrodes, where DNA duplexes containing a tethered alkanethiol are attached to a gold electrode passivated with β -mercaptohexanol, can be used to assess redox signals from DNA-bound, [4Fe4S] proteins (yellow, left). Signals are attenuated when base lesions (red, center) in the duplex are present, or when the redox pathway within the [4Fe4S] protein, as for Y82A (gray, right) is deficient in CT. Cyclic voltammetry (below, left) scanning can be used to measure the DNA-mediated redox signal from CT-proficient proteins (WT EndoIII, blue) and CT-deficient proteins (EndoIII Y82A, red). A multiplexed chip platform (below, right) has now been adapted to measure [4Fe4S] protein signals on 16 separate DNA-modified electrodes, with replicates on a single surface (32, 48-50).

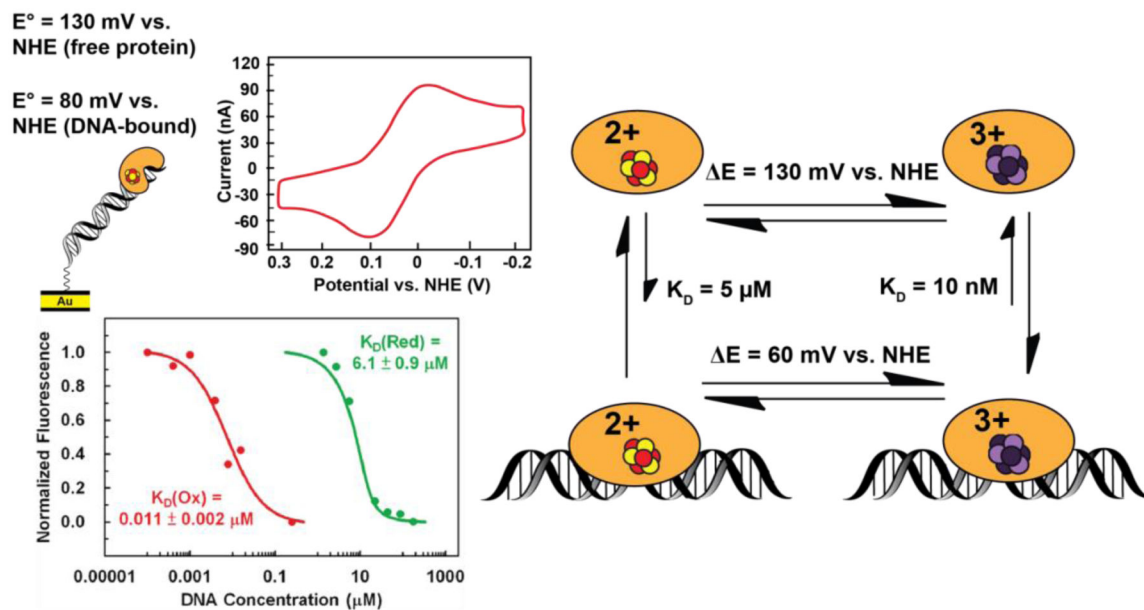


Figure 5. DNA binding shifts the potential of [4Fe4S] cluster enzymes.

Endonuclease III has a redox potential of approximately 80mV vs. NHE for the $[4\text{Fe}4\text{S}]^{3+/2+}$ couple measured on a DNA-modified Au electrode. (Above, left) This potential is a negative shift from the ~130mV vs. NHE potential for this couple when the protein is not bound to DNA. This shift corresponds thermodynamically to a stabilization of the oxidized $[4\text{Fe}4\text{S}]^{3+}$ state upon binding the DNA polyanion (right). Microscale thermophoresis on electrochemically oxidized and native reduced Endonuclease III (below, left) indicates that a ~550-fold increase in DNA binding affinity is associated with the conversion from $[4\text{Fe}4\text{S}]^{2+}$ to the $[4\text{Fe}4\text{S}]^{3+}$ state, (53) consistent with this negative shift in potential.

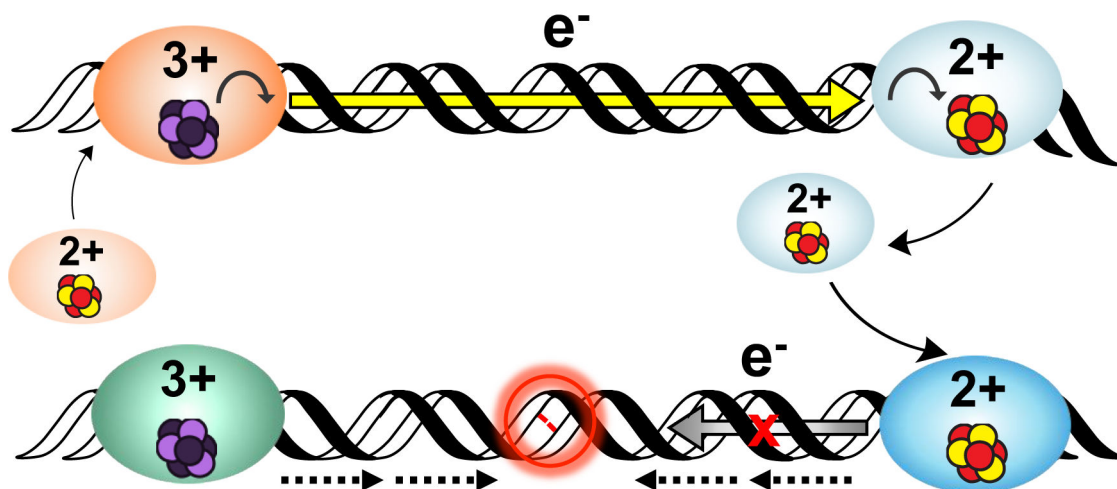


Figure 6. A model for DNA-mediated redox signaling between repair proteins.

Enzymes with the cluster in the native $[4\text{Fe}4\text{S}]^{2+}$ state first bind DNA, causing the cluster to become activated toward oxidation. Oxidative stress initiates the damage search when highly reactive species such as the guanine radical cation are formed; these can oxidize DNA-bound proteins in their vicinity. Oxidation of the cluster to the $[4\text{Fe}4\text{S}]^{3+}$ state leads to a > 500-fold increase in DNA binding affinity, so oxidized proteins remain bound and diffuse along the DNA. Another $[4\text{Fe}4\text{S}]^{2+}$ protein bound at a distant site can reduce the oxidized protein, effectively scanning the intervening DNA for lesions through DNA-mediated CT. At this point, on damage-free DNA (above) the reduced protein binds less tightly to DNA and can diffuse away, while the newly oxidized protein continues the damage search. This process of redox exchange continues until a segment of DNA containing a lesion is approached. Since even subtle lesions can disrupt base stacking (below), CT is attenuated and any nearby oxidized proteins remain bound. Thus, DNA CT allows repair proteins to scan large sections of the genome and redistribute to areas containing damage (24, 37).

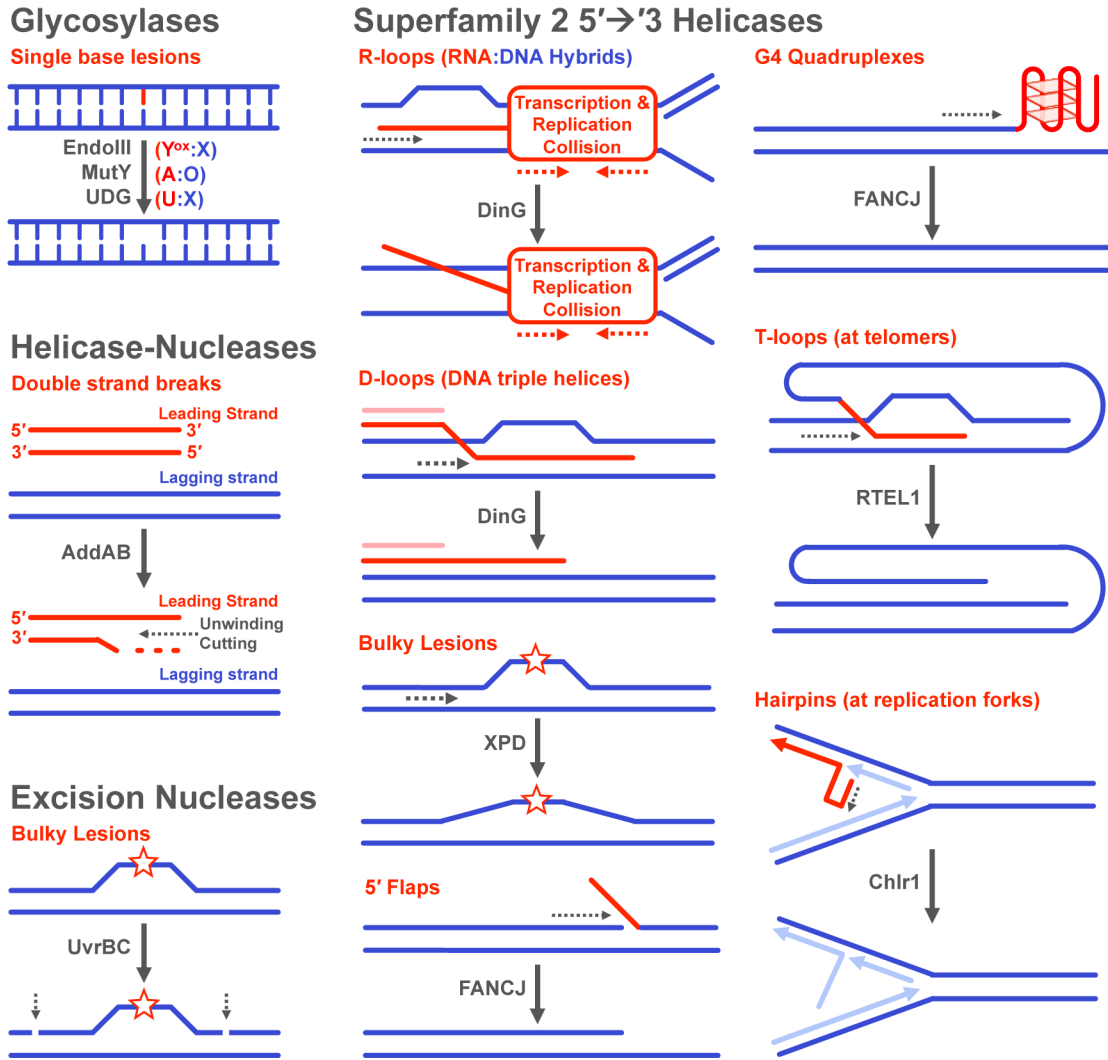
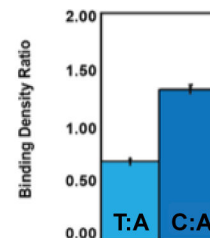
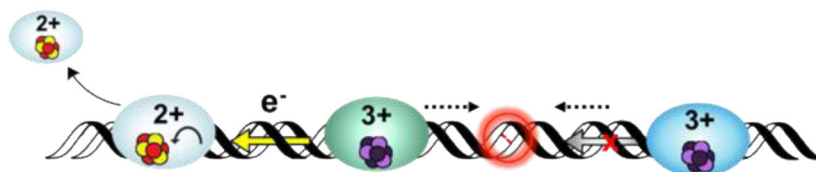


Figure 7. Reactions and Substrates for DNA repair enzymes containing [4Fe4S] clusters. (Top, left) Glycosylases remove a number of single-base lesions caused by endogenous and exogenous agents. (Middle, left) The helicase-nuclease AddAB processes double strand breaks. (Bottom, left) The UvrBC complex cleaves the phosphodiester backbone around the damaged strand of DNA. (Right) Superfamily 2 5'→3' helicases participate in a number of pathways and are involved in unwinding very diverse substrates. The substrate specificity is overlapping for many of the helicases (ex. FANCI and RTEL1), though genome location (ex. telomeres) and cell cycle phase (ex. replication in the S phase) appear to be factors in activity (73, 77, 81, 82, 87, 91,93).

Enhanced Lesion Detection



Impaired Lesion Detection

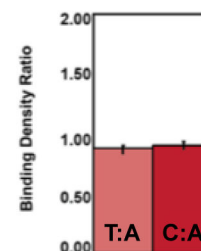
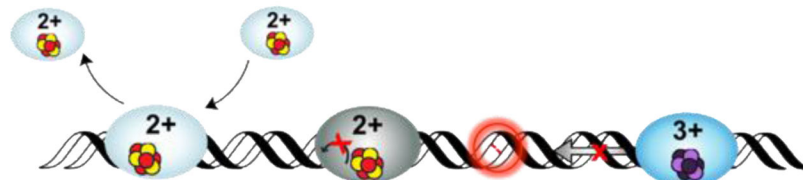


Figure 8. Visualization of Protein Localization on Damaged DNA by Atomic Force Microscopy (AFM).

In the AFM redistribution assay, [4Fe4S] protein or protein mixtures are incubated with DNA substrates which contain either long, well matched DNA strands (3.8 kb) or strands containing a single C:A mismatch in the 3.8 kb duplex along with short, undamaged DNA strands (1.6 and 2.2 kb). Images are collected and proteins bound to long strands of DNA are counted, normalized to the proteins bound to the short strands, and expressed as a binding density ratio (right). As shown at right (top), a greater density of proteins is found on the strands containing a mismatch (C:A) compared to the well-matched (T:A) strand, even though the repair proteins do not bind the C:A mismatch as a substrate. If the protein is defective in carrying out DNA CT, however, the binding density is the same on the mismatched and matched strands (bottom right) (55, 59, 79, 80).

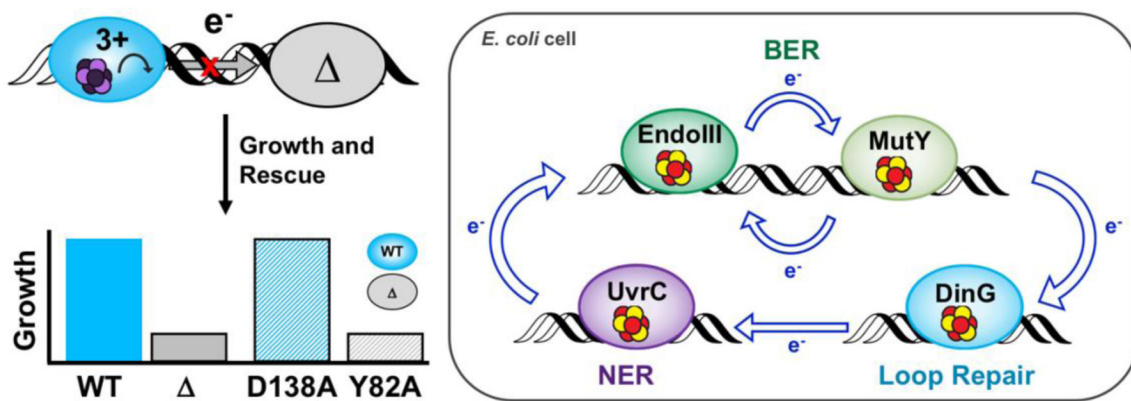


Figure 9. Genetic Assays for Detection of DNaCT Signaling Among *E. coli* [4Fe4S] Repair Proteins.

(Top left) *E. coli* parent (blue) and EndoIII knockout (KO, gray) strains that report on the repair protein activity have been used to monitor DNA-mediated communication between putative signaling partners *in vivo*. Complementation plasmids expressing CT-proficient (D138A) or CT-deficient (Y82A) versions of EndoIII are introduced to EndoIII KO strains to evaluate if the parent phenotype can be rescued (bottom left). Rescue can only be achieved with a CT-proficient enzyme (blue bar, gray outline), strongly indicating that DNA-mediated redox signaling is necessary for efficient repair. (Right) The redox signaling network in *E. coli* includes BER, loop repair, and NER (57, 59, 79, 80).

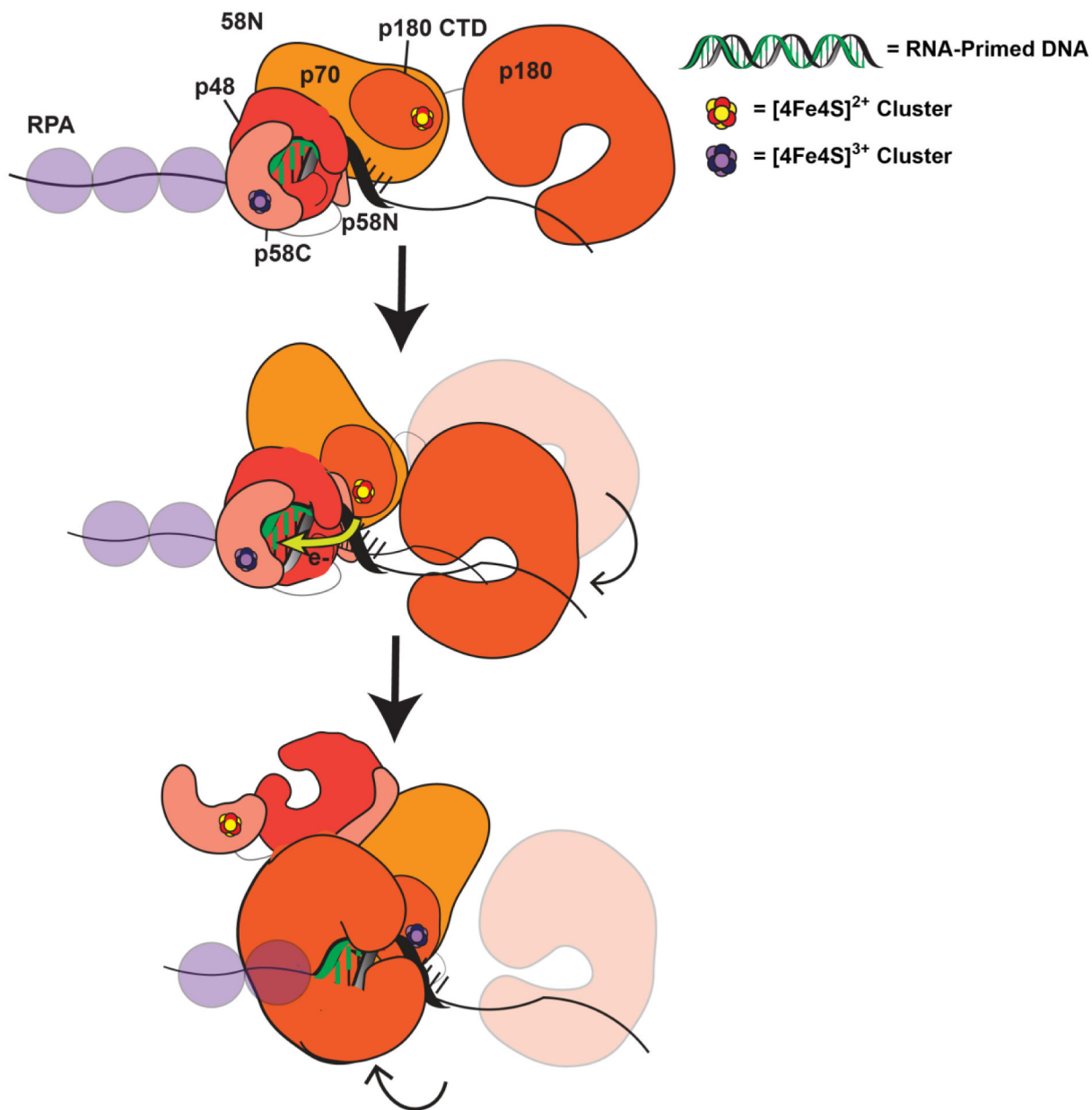


Figure 10. Model for primase-polymerase α handoff through redox switching.

(52) Oxidized $[4Fe_4S]^{3+}$ primase is bound to the RNA/DNA primer during primer synthesis. Polymerase α is DNA-dissociated and reduced but flexibly tethered to primase (Top). When the RNA primer reaches appropriate length, polymerase α orients in a manner coupling the $[4Fe_4S]$ cluster into the RNA/DNA substrate and can be oxidized by DNA CT through this segment, sending an electron through the primed template to reduce DNA primase (Middle). Reduced primase dissociates from the RNA-primed DNA, and oxidized polymerase α can then synthesize DNA downstream of the primase product (Bottom).

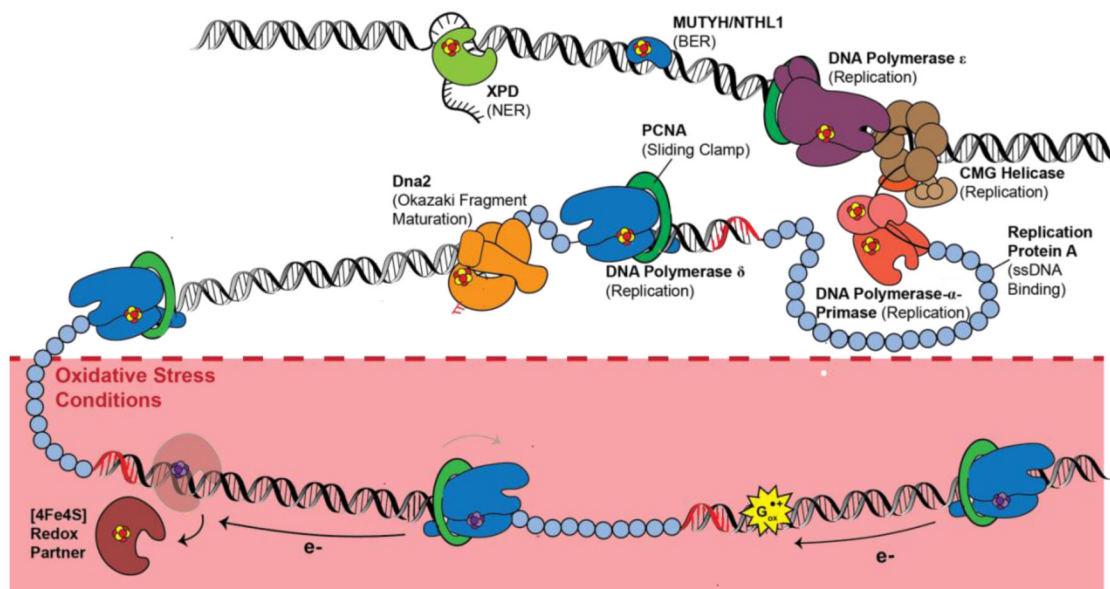


Figure 11. [4Fe4S] enzymes in eukaryotic repair and replication.

B-family polymerases, DNA primase, Dna2 helicase-nuclease, BER/NER enzymes such as MUTYH, NTHL1, and XPD, all coordinate a [4Fe4S] cluster cofactor. Several of these proteins have been demonstrated to participate in DNA-mediated redox signaling; characterization of their redox roles is ongoing. (Below) Under oxidative stress conditions, polymerase δ may be converted to the [4Fe4S]³⁺ state as a means to stall synthesis under poor cellular conditions. Polymerase δ can be reversibly oxidized and reduced through DNA CT, which may regulate polymerase activity on the lagging strand.

Table 1.
DNA-processing, [4Fe4S] enzymes are found in prokaryotes, archaea, and eukaryotes.

These enzymes are found in different pathways, such as repair, replication, and transcription, and perform specialized, distinct tasks in cells.

[4Fe4S] Protein	Pathway		Function	Reference
	Bacteria	Eukarya		
Endonuclease III		NTHL1, Nig2	Bifunctional glycosylase, removal of oxidized pyrimidine bases	12,24
MutY		MUTYH	Glycosylase, removes adenines mispaired with 8-oxo-guanine	22,24,58
DinG	XPD	XPD, Rad3	5'-3' helicase, unwinds DNA surrounding TT dimers	65,97
			Helicase, unwinds R-loop structures	64
		FANCI	5'-3' helicase, generates ssDNA overhangs for homologous recombination	65
AddAB		RteI, ChlI	5'-3' helicase, unwinds specialized DNA structures	83,89
			Helicase-nuclease with 5'-3' nuclease activity, generates 3'-ssDNA overhangs	90
		Dna2	Helicase-nuclease, ssDNA-dependent ATPase, Okazaki fragment processing/double-strand break repair	107
		DNA Primase	DNA-dependent RNA polymerase, synthesizes 8-14nt RNA primer on ssDNA	62,63
		DNA Polymerase α	Extends RNA primer by 10-20nt	106
		DNA Polymerase δ	Lagging Strand DNA polymerase, 3'-5' exonuclease	106
		DNA Polymerase ϵ	Leading Strand DNA polymerase, 3'-5' exonuclease	106, 124
		DNA Polymerase ζ	Translesion synthesis polymerase	106, 124, 134
Cas4	RNA Polymerase	Elp3	Template-directed RNA synthesis	24,29
PhrB			5'-3' exonuclease	26
UvrC			Repair of UV-induced cyclopyrimidine dimers	25
Spore Photoproduct Lyase			5'-3' endonuclease	28
			(5R)-5-(α -thymyl)-5,6-dihydrothymidine lesion repair	30